



Cite this: *RSC Chem. Biol.*, 2021, 2, 685

Received 3rd February 2021,  
Accepted 2nd March 2021

DOI: 10.1039/d1cb00023c

rsc.li/rsc-chembio

## Nanobodies as *in vivo*, non-invasive, imaging agents

Thibault J. Harmand,<sup>id</sup><sup>a</sup> Ashrafal Islam,<sup>id</sup><sup>ab</sup> Novalia Pishesha<sup>acd</sup> and  
Hidde L. Ploegh<sup>id</sup><sup>\*a</sup>

*In vivo* imaging has become in recent years an incredible tool to study biological events and has found critical applications in diagnostic medicine. Although a lot of efforts and applications have been achieved using monoclonal antibodies, other types of delivery agents are being developed. Among them, VHHs, antigen binding fragments derived from camelid heavy chain-only antibodies, also known as nanobodies, have particularly attracted attention. Indeed, their stability, fast clearance, good tissue penetration, high solubility, simple cloning and recombinant production make them attractive targeting agents for imaging modalities such as PET, SPECT or Infra-Red. In this review, we discuss the pioneering work that has been carried out using VHHs and summarize the recent developments that have been made using nanobodies for *in vivo*, non-invasive, imaging.

### 1. Introduction

*In vivo* imaging allows the investigation of molecular and cellular events in intact living subjects. Studying the dynamics of biological processes non-invasively and in their native context may offer new

insights and provide opportunities for the discovery of novel biology. *In vivo* imaging has therefore become an indispensable tool in both biomedical research and medical practice.<sup>1–5</sup>

A diverse set of *in vivo* imaging approaches has been developed. These include Positron Emission Tomography (PET), Single Photon Emission Computed Tomography (SPECT), Computed Tomography (CT), Magnetic Resonance Imaging (MRI), Infra-Red and Near Infra-Red Imaging (IR/NIR), Ultrasound (US), and photoacoustic imaging.<sup>1,3–8</sup>

Regardless of the method used, *in vivo* imaging requires differential accumulation of the relevant signal at the target site to distinguish it from background.<sup>9</sup> The major challenge of

<sup>a</sup> Program in Cellular and Molecular Medicine, Boston Children's Hospital, Harvard Medical School, Boston, MA, USA. E-mail: hidde.ploegh@childrens.harvard.edu

<sup>b</sup> Department of Clinical Medicine, UiT The Arctic University of Norway, Tromsø, Norway

<sup>c</sup> Society of Fellows, Harvard University, Cambridge, MA, USA

<sup>d</sup> Klarman Cell Observatory, Broad Institute of MIT and Harvard, Cambridge, MA, USA



Thibault J. Harmand

Thibault Harmand received his PhD in organic chemistry from the ETH Zürich under the supervision of Prof. Jeffrey Bode where he worked on the total chemical synthesis of proteins. He joined the lab of Dr Hidde Ploegh as a postdoctoral fellow with a fellowship from the Swiss National Science Foundation in 2017. In the Ploegh lab he has been working on bioconjugation methods to modify peptides, biomolecules and living cells to study biology and develop novel therapies.



Ashrafal Islam

Dr Ashrafal Islam earned a Bachelor of Pharmacy (2008) from Northern University Bangladesh. He received an MSc in Biomedicine (2013) and a PhD in Cell Biology (2018) from UiT The Arctic University of Norway. In 2019, he moved to Boston Children's Hospital/Harvard Medical School, where he works as a postdoctoral fellow (grant from the Norwegian Cancer Society and an overseas grant from UiT) in the Ploegh lab. Currently, he is performing a PET imaging project, with an emphasis on scFv-based PET tracer development, to investigate the infiltration of immune cells into the tumor microenvironment.



non-invasive *in vivo* imaging of a target of interest is to achieve adequate selectivity and discrimination from the background signal in the targeted area. To achieve specificity, combining the imaging agent (radio)isotope or fluorophore with a carrier such as antibodies,<sup>10</sup> peptides,<sup>11,12</sup> small molecules,<sup>13</sup> and aptamers<sup>14,15</sup> has been the method of choice. In particular, immunoglobulins and immunoglobulin-derived fragments have long been considered attractive candidates, since they can be generated to target a wide range of biomolecules<sup>16–18</sup> and recognize them with exquisite specificity.

Nevertheless, monoclonal antibodies (mAbs) are large (150 kDa), which explains their comparatively poor tissue penetration when administered systemically, with a long circulatory half-life.<sup>9,19</sup> Efforts have been devoted to improving the pharmacokinetics of antibodies without compromising their unique affinity and specificity. Antibody fragments such as Fab, F(ab')<sub>2</sub>, single chain Fv (scFv), or variants like diabodies and minibodies (molecular weight ranging from 25–100 kDa) were bioengineered specifically for the purpose of creating *in vivo* imaging agents.<sup>20–22</sup> More recently, other types of proteins have been investigated as alternatives to antibodies for *in vivo* imaging. These include nanobodies (Fig. 1), Affibodies, and anticalins.<sup>20–22</sup>

Of these, nanobodies have attracted growing interest for use in molecular imaging across various imaging platforms, including SPECT, PET, Infra-red (IR) and ultrasound.<sup>9,23</sup>

Nanobodies are antigen binding fragments derived from camelid heavy chain-only antibodies, which fold and function in the absence of light chains. These camelid immunoglobulin (Ig) heavy chains can be shrunk to just their variable domains to yield VHHs or nanobodies. The resulting VHHs retain antigen binding and can be produced in an active form in *E. coli*, often without the need of an intrachain disulfide bond. Typically, nanobodies have a molecular weight of ~12–16 kDa and are considered the smallest immunoglobulin-derived antigen binding fragments.<sup>24</sup> Because of their much smaller size when compared to intact Ig (~150 kDa), Fab (~50 kDa) and scFv (~25 kDa) fragments, nanobodies can

penetrate tissues more efficiently and bind to antigens less accessible to conventional antibodies or their smaller derivatives.<sup>19,25–27</sup> Better tissue penetration is not the only advantage of nanobodies as compared to intact conventional Ig. Nanobodies are poorly immunogenic in humans,<sup>19</sup> and some nanobodies have been “humanized” to display even less immunogenicity.<sup>25,28,29</sup> Furthermore, their small size and the preponderance of beta sheet secondary structure make them highly stable, even at high temperatures and extremes of pH.<sup>30</sup> Finally, owing to their small size, nanobodies that fail to bind their target are rapidly cleared from the blood, mostly by renal elimination.<sup>19,25,31–34</sup> This, in tandem with their usually high affinity, can produce a high tumor-to-background ratio as early as 1 h after tracer injection.<sup>32,35,36</sup>

Although nanobodies possess the many advantages listed above, their relatively small size leads to rapid elimination from the circulation by renal clearance. Their rapid renal clearance from the body might prevent optimal binding at the desired site,<sup>35</sup> as the concentrations of the imaging agent in the circulation drop rapidly. This is often accompanied also by uptake of the imaging agent in the kidneys, making imaging experiments in neighboring tissues difficult because of the high background.<sup>37</sup> Finally, the binding properties of nanobodies may be altered when they are conjugated to produce imaging agents.<sup>38</sup>

In this review, we describe how nanobodies are equipped with the corresponding probes for each imaging modality and how rapid clearance and non-targeted organ uptake, problems inherent in the use of nanobodies, can be overcome.

## 2. Labeling of nanobodies for *in vivo* imaging

In order to be observable by any imaging modality (SPECT, PET, or IR), nanobodies must be equipped with a suitable radioisotope or fluorescent dye. Although some aspects of the



**Novalia Pishesha**

*Dr Novalia Pishesha completed her BS in Bioengineering from the University of California at Berkeley and her PhD in Biological Engineering from Massachusetts Institute of Technology. Since 2018, she has been a Junior Fellow at the Harvard Society of Fellows. In the Ploegh lab, her project revolves around developing engineered proteins and cells to investigate and tackle auto-immune diseases and infectious diseases.*



**Hidde L. Ploegh**

*Hidde Ploegh is a biochemist interested in questions of immunological relevance. He trained with Jack Strominger at Harvard University and has held positions at the University of Cologne and the Netherlands Cancer Institute. He joined the MIT faculty in 1992, and in 1997 joined Harvard Medical School, where he directed the graduate program in immunology. In 2005 he returned to MIT at its Whitehead Institute. In 2016 he joined the Program in Cellular and Molecular Medicine at Boston Children's Hospital, where he continues to explore the properties and applications of nanobodies. His interests include chemo-enzymatic approaches to protein modification.*





Fig. 1 Schematics of the different antibodies and antibody fragment structures.

requisite methods for modification are similar, the imaging modality chosen might require specific considerations with respect to the labeling method used.

### 2.1. Radio-labeling for SPECT and PET imaging

Radiohalogens, like  $^{123/125/131}\text{I}$  for SPECT or  $^{124}\text{I}$  and  $^{18}\text{F}$  for PET, must be covalently attached to the nanobody. Radiometals such as  $^{67}\text{Ga}$ ,  $^{99\text{m}}\text{Tc}$ , and  $^{111}\text{In}$  for SPECT and  $^{64}\text{Cu}$ ,  $^{68}\text{Ga}$ , and  $^{89}\text{Zr}$  for PET are complexed *via* a chelator and thus require a two-step process where the nanobody is first equipped with a chelator and then incubated with the radiometal in solution. The (His)<sub>6</sub> tag often present on recombinantly expressed proteins to facilitate affinity purification readily coordinates site-specifically with  $^{99\text{m}}\text{Tc}$ -tricarbonyl.<sup>39,40</sup>

In either case, a chelator or a prosthetic group must be attached to the nanobody of choice. Various labeling approaches can be divided into two major classes: uncontrolled or site-specific labeling. Uncontrolled labeling relies mainly on lysine and cysteine conjugation *via* carbodiimide/*N*-hydroxy-succinimide (DIC/NHS) chemistry or maleimide chemistry, respectively. Although this method is common, straightforward, and easily accessible, the heterogenous mixture of labeled products might lead to reduced binding of the nanobody, especially if the binding site itself is modified.<sup>41</sup> Site-specific strategies aim to obtain homogeneous and more consistent products, with the desired moiety attached to a specific site of one's choosing. Different site-specific methods to modify nanobodies have been described, relying on enzymatic methods, click chemistry, or meticulous and selective incorporation of an unpaired cysteine residue.<sup>24,42</sup>

There are a wide range of commercially available chelators with functionalized handles, such as maleimide, NHS ester, azido derivatives, *etc.* (Fig. 2A). However, this is not the case for the radiohalogens (obtained as salts) for both  $^{18}\text{F}$  and  $^{123/124/125/131}\text{I}$ . The Iodogen method allows rapid but uncontrolled iodination of the desired protein *via* an oxidation reaction of tyrosine sidechains, but a more sophisticated synthetic chemistry is required to prepare radiohalogen reagents prior to their use for the labeling of nanobodies (Fig. 2B).<sup>43,44</sup>

### 2.2. Fluorescent dye labeling for IR and NIR

*In vivo* imaging using fluorescent dyes relies on fluorophores emitting in the near infrared (NIR) or infrared region (IR). An ideal dye should have a maximum emission in the 650 nm to 900 nm range (Fig. 2C). This particular range of wavelengths reduces scattering and nonspecific autofluorescence, produces a good signal to background ratio, and thus improves resolution.<sup>23</sup> The cyanine dye derivatives: Cy5, AF680, IRDye 680RD, IRDye800CW, *etc.* are commonly used for this application.<sup>45,46</sup> However, their high hydrophobicity has pushed the development of more water-soluble dyes, such as the pyrrolopyrrole cyanine family (PPCy) (Fig. 2C).<sup>47</sup>

Conjugation of fluorophores can significantly affect pharmacokinetics, biodistribution, quality/stability and aggregation properties of the engineered construct. Uncontrolled and multiple-labeling of fluorophores to nanobodies yields products with abnormal distribution, can contribute adversely to the background signal, produces accumulation in non-targeted organs such as the liver and results in poor contrast for the target of interest.<sup>36,48–51</sup> Site-specific labeling of IRDye800CW





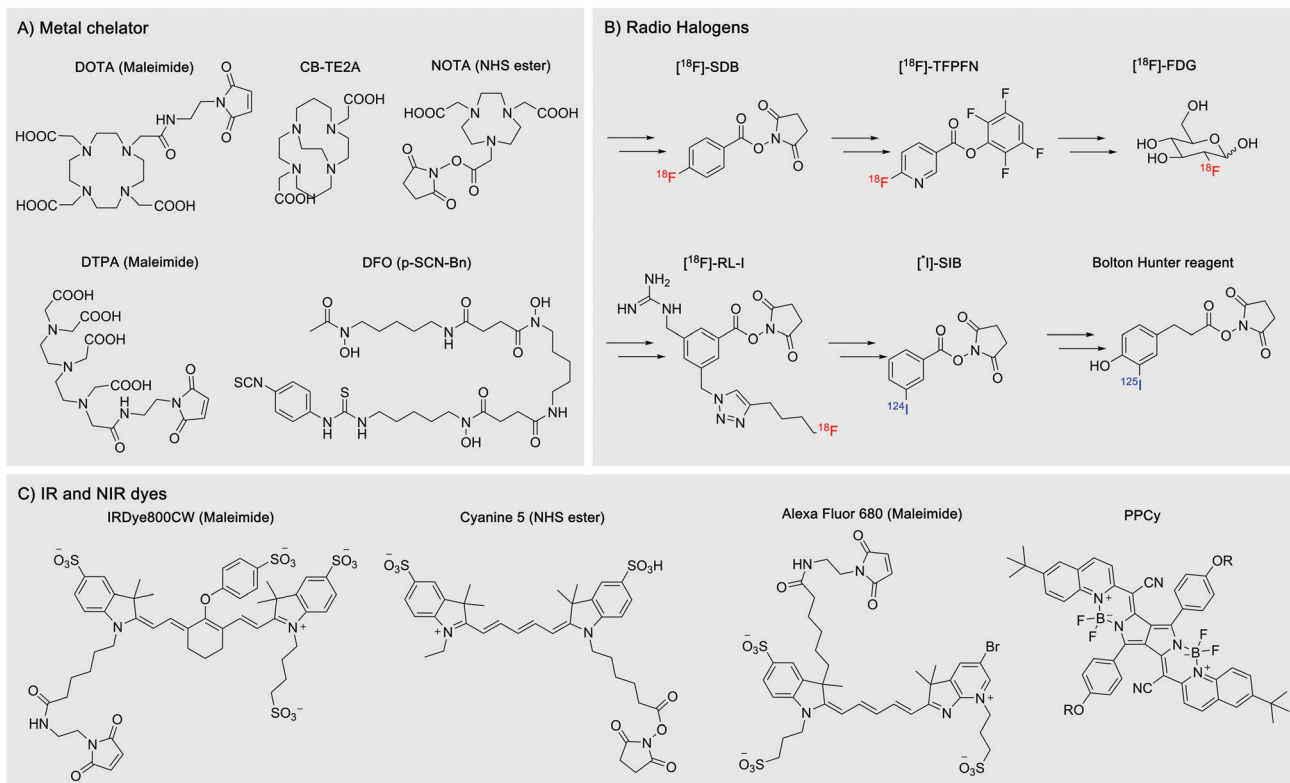


**Fig. 2** Examples of potential probes for *in vivo* labeling. Most of them are commercially available as maleimide, NHS ester, azide, etc. derivatives. (A) Metal chelators used for SPECT and PET imaging. (B) Typical radio halogen-based reagents. (C) IR and near IR dyes for infra-red imaging.

and IRDye680RD dyes by conjugation to a selectively introduced C-terminal cysteine yields imaging agents with improved biodistribution: acceptable kidney uptake, rapid binding to the target of interest and minimal nonspecific uptake (Fig. 3).<sup>49</sup>

Nanobodies for NIR/IR *in vivo* imaging can also be prepared as fusions to a far-red fluorescent protein. This eliminates the need of further handling of the nanobody but comes with a drawback: the considerable size of the fluorescent protein (20–30 kDa) compared to the nanobody (~15 kDa) might disturb binding and the biodistribution of the resulting fusion protein.<sup>23,51</sup>

### 3. Overcoming nanobody challenges: renal accumulation and rapid clearance

Long-term renal retention of nanobodies, especially in a radiolabeled form, can cause nephrotoxicity. The bright kidney signals caused by such accumulation make the imaging of molecular targets in the adjoining areas difficult. Different strategies have been developed to reduce renal absorption. For example, co-injection with gelofusin or positively charged

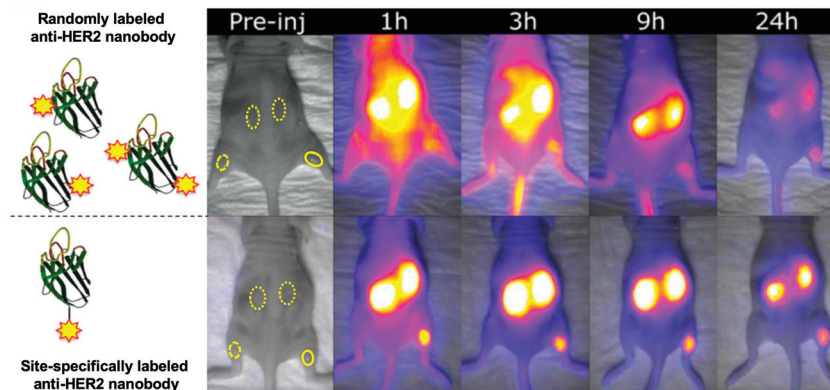


**Fig. 3** Effects of the unspecific conjugation of NIR/IR dye on the biodistribution of a nanobody (solid ROI: tumor; dashed ROI: contra-lateral muscle; dotted ROI: kidney). In this tumor mouse model, the anti-HER2 nanobody (2Rs15d) was labeled with IRDye800CW in an uncontrolled and controlled manner (top and bottom panel respectively). Adapted with permission from.<sup>49</sup> Copyright (2017) American Chemical Society.



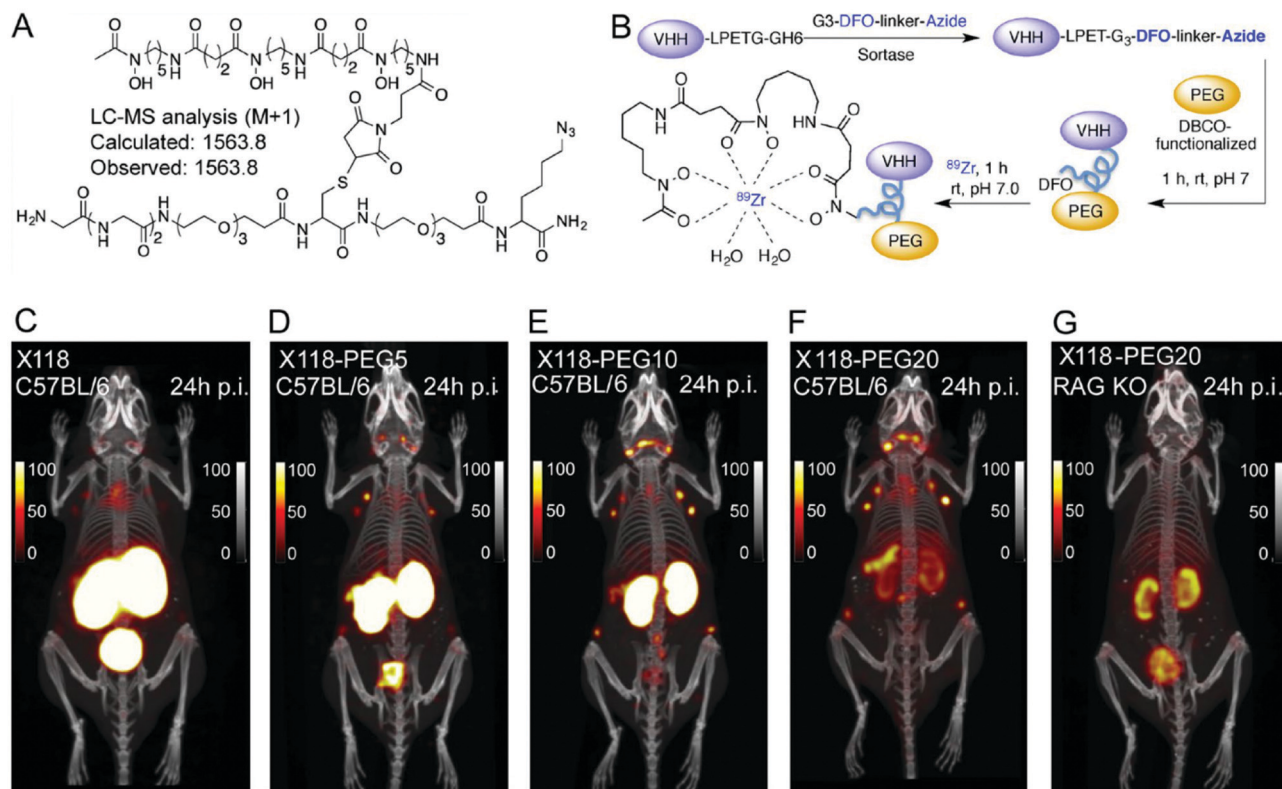


**Fig. 4** Selective labeling, using sortase A, of a nanobody with a metal chelator for  $^{89}\text{Zr}$ -based PET imaging. (A) Structure of the bioorthogonal sortase substrate. (B) Schematic representation of preparing PEGylated  $^{89}\text{Zr}$ -labeled VHHs for PET imaging. (C–G) PET-CT images of anti-CD8  $^{89}\text{Zr}$ -labeled (VHH $_{\text{X118}}$ ) with and without different-size PEG in wild-type C57BL/6 and RAG $^{-/-}$  mice. Images were acquired 24 h post-injection of the radiolabeled VHHs. Adapted from ref. 56.

amino acids like lysine can reduce renal uptake for radio-labeled biomolecules.<sup>52,53</sup> This strategy has also been applied to nanobodies.<sup>31,54</sup> Another approach consists of removing the affinity tags often used for purification purposes: these tags, typically myc or (His)<sub>6</sub> tags, consist of negatively- and positively-charged amino acids respectively, and can directly impact the degree of renal accumulation of the nanobody.<sup>54,55</sup> Attachment of PEG moieties can decrease renal uptake. The availability of differently sized PEGs allows simple screening and tuning of the desired construct to optimize its imaging characteristics. Rashidian *et al.* used nanobody constructs bearing differently sized PEG moieties and showed a direct correlation between the size of the PEG moiety and the amount of tracer accumulating in the kidney (Fig. 4).<sup>56</sup>

Unmodified VHH X118, a nanobody that targets CD8<sup>+</sup>T cells, fails to cleanly show the spleen (located near the kidneys), although the spleen is a main reservoir of CD8<sup>+</sup>T cells. In contrast, the 20 kDa PEG-derivative of VHHX118 readily allows visualization of secondary lymphoid organs.

PEGylation tackles yet another variable associated with the use of nanobodies, which is their rapid clearance from the circulation. While quick elimination from the body allows nanobodies to be used for same-day imaging, it also can lead to poor accumulation in the area of interest. Attachment of PEG of different sizes, *e.g.* 5, 10 or 20 kDa, increases their molecular

weight/Stokes' radius and thus their circulatory dwell time, with an improvement in the signal to noise ratio.<sup>56</sup> Increasing the half-life of nanobodies by increasing their size has been accomplished by methods other than PEGylation. Wardners *et al.* used a tri-paratopic nanobody construct, consisting of two nanobodies that bind to two different HER3 epitopes and a third that binds to albumin in order to extend the circulatory half-life of the construct. This construct showed less renal accumulation than a 'regular' HER3-targeting nanobody and circulated longer, as measured by radioactivity remaining in the blood.<sup>57</sup> Size and targeting properties must be properly balanced, parameters that cannot be predicted and therefore require systematic experimentation.

Interestingly, the degree of kidney retention for radiohalogenated (fluorinated and iodinated) nanobodies is significantly lower than their radiometal-labeled counterparts. Catabolites of radiohalogenated compounds formed in the kidneys are thought to be non-residualizing and hydrophobic. They are rapidly excreted *via* the urine.<sup>23</sup>

With the exception of this kidney accumulation – which can be overcome at least in part by the methods described here – accumulation in other non-targeted organs is usually very low. The unique characteristics of nanobodies (efficient tissue penetration, fast tissue diffusion and fast clearance) thus allow same-day imaging with high target-to-background ratios.<sup>9,23</sup>



This is impossible to achieve with conventional antibodies, where several days of equilibration between circulation and target tissues are required after administration before it is possible to acquire high quality images.

## 4. Application and examples of nanobodies for *in vivo* imaging

### 4.1. Radio imaging: SPECT and PET

Radionuclide-based techniques such as PET and SPECT are commonly used because they are sensitive, quantitative, and clinically relevant.<sup>58,59</sup> SPECT and PET have the sensitivity needed to visualize most interactions between physiological targets and ligands, enabling non-invasive detection of tracers down to the picomolar level.

**4.1.1. SPECT imaging using nanobodies.** Single-photon imaging exploits the  $\gamma$  rays emitted by a radioactive atom. A  $\gamma$ -emitting element with an energy of 100–250 keV is ideal.<sup>1</sup> The spatial resolution of single-photon imaging is on the order of 8–10 mm, although somewhat better resolution can be obtained with recently developed special-purpose imaging systems.<sup>60–63</sup>

Although <sup>99m</sup>Tc, <sup>123/131</sup>I, <sup>111</sup>In and <sup>155</sup>Tb are the four radionuclides suitable and commonly used for SPECT imaging,<sup>64</sup> only two of them have been used with nanobodies: <sup>99m</sup>Tc and <sup>111</sup>In. A few examples describe nanobody-based SPECT imaging using <sup>111</sup>In as a radionuclide: Chatalic *et al.* developed an anti-PSMA nanobody conjugated to the metal chelator diethylenetriaminepentaacetic acid (DTPA), which showed good tumor targeting and minimal uptake by the non-targeted organs.<sup>54</sup> Bala *et al.* used <sup>111</sup>In in combination with a VCAM-1 targeting nanobody in a study to compare the pharmacokinetics of the imaging agent with the use of the different tracers: <sup>68</sup>Ga, <sup>18</sup>F, <sup>111</sup>In and <sup>99m</sup>Tc.<sup>65</sup>

The reason for the success of <sup>99m</sup>Tc as a radionuclide for SPECT imaging derives not only from its favorable nuclear decay characteristics, but also from its simple and straightforward radiolabeling chemistry. This has allowed the labeling of a wide range of biomolecules. For example, <sup>99m</sup>Tc(CO)<sub>3</sub> can be used to directly label nanobodies equipped with a (His)<sub>6</sub> tag without further modifications.<sup>32,66</sup> Additionally, the long half-life of <sup>99</sup>Mo and the low cost associated with the <sup>99</sup>Mo/<sup>99m</sup>Tc generator make the production of <sup>99m</sup>Tc widely available.<sup>67</sup>

Nanobodies against many different markers have been used in combination with <sup>99m</sup>Tc for SPECT imaging of cancers. Examples include epidermal growth factor receptor 1 (EGFR)<sup>31,32,66,68,69</sup> and 2 (HER-2),<sup>70</sup> prostate-specific membrane antigen (PSMA),<sup>71</sup> the Macrophage Mannose Receptor (MMR),<sup>37</sup> carcinoembryonic antigen (CEA),<sup>72,73</sup> mesothelin<sup>74</sup> and the M-protein.<sup>75</sup> Nanobodies that target non-cancer markers have also found application for SPECT imaging. De Vos *et al.* immunized a dromedary with the Lectin-like oxidized low density lipoprotein receptor (LOX-1).<sup>76</sup> This protein is a biomarker for detection and phenotyping of atherosclerotic plaques. They obtained a nanobody, LOX-sdAb, that binds LOX-1 with picomolar affinity. Recombinant expression in *E. coli* of

this nanobody equipped with a C-terminal (His)<sub>6</sub>-tag, followed by direct radiolabeling using <sup>99m</sup>Tc(CO) allowed SPECT imaging in apolipoprotein E-deficient mice (ApoE<sup>−/−</sup>). It showed a clear signal of atherosclerotic plaques in the aortic arch. This nanobody is an example of a potentially powerful tool for cardiovascular prognostic and diagnostic use.

Other examples of diseases/conditions imaged using nanobodies for SPECT include diabetes,<sup>77,78</sup> liver inflammation,<sup>79,80</sup> rheumatoid arthritis,<sup>81,82</sup> Gelsolin amyloidosis,<sup>83</sup> imaging of immune cells,<sup>84</sup> or more generally immune checkpoints in cancer.<sup>85</sup> Nanobodies used for SPECT imaging, labeled with <sup>99m</sup>Tc, are summarized in Table 1 and show the breadth of nanobodies deployed for such studies.

While these preclinical examples show the utility of nanobodies for SPECT imaging in mouse models, their application for *in vivo* imaging in humans is not as straightforward. Nanobodies, because of their non-human origin, might induce an immune response when applied in clinical settings. “Humanization” of nanobodies is usually considered to advance their application to the clinic. Vaneycken *et al.* described an interesting approach in which they genetically grafted the CDRs of an anti-CEA nanobody, NbCEA5, onto a humanized nanobody scaffold (Fig. 5).<sup>73</sup>

The “transplant” was successful, and the grafted nanobody displayed imaging properties similar to the original. This promising work opens the door to wider application of nanobodies in a human setting.

**4.1.2. PET imaging using nanobodies.** PET is considered the more attractive non-invasive imaging modality over its single-photon cousin, owing to its higher spatial resolution (usually 2–3 mm or lower for PET), higher sensitivity (typically 10<sup>−8</sup> to 10<sup>−10</sup> M tracer concentrations for PET, compared to ~10<sup>−6</sup> M for SPECT), and the wide availability of positron-emitting radioisotopes.<sup>90</sup> In the context of immuno-oncology, nanobodies and PET have been partnered to investigate the expression and tracking of immunologically relevant molecular targets, such as effector molecules, immune cell populations, and checkpoint molecules within the tumor microenvironment (TME). The application of nanobodies to cancer-relevant models, both for imaging and therapeutic purposes has been reviewed recently,<sup>9,23,91,92</sup> but some highlights are presented in the following.

Nanobody-based PET tracers that target cancer biomarkers, such as human epidermal growth factor receptor 2 (HER2),<sup>33,93,94</sup> HER3,<sup>57</sup> CD20,<sup>95</sup> epidermal growth factor receptor (EGFR)<sup>34</sup> and hepatocyte growth factor (HGF),<sup>96</sup> have been used as imaging agents to evaluate the presence or absence of these biomarkers in preclinical models. The results from these studies showed high tumor-specific uptake of the nanobody-based probes into the TME. A major step towards clinical translation of nanobody-based PET tracers was the phase I clinical trial of <sup>68</sup>Ga-NOTA-labeled anti-HER2 nanobody in breast carcinoma patients.<sup>97</sup> PET/CT images taken at 90 min post-injection were chosen as the optimal imaging time point, showing less background than at earlier time points. Irrespective of non-specific accumulation of tracer in the liver, kidneys





Table 1 Overview of nanobody-based tracers for non-invasive SPECT imaging using  $^{99m}\text{Tc}$ 

| Condition            | Target     | Nanobody                   | Disease model  | Ref.          |
|----------------------|------------|----------------------------|--|---------------|
| Cancer               | EGFR       | D10                        | Human epidermoid carcinoma (A431)  | 66            |
|                      |            | 7C12                       | Human epidermoid carcinoma (A431),<br>human prostate carcinoma (DU145)                                   | 31, 68 and 69 |
|                      |            | 8B6                        |  | 32            |
|                      | PSMA       | PSMA30                     | Prostate cancer (LNCaP)  | 71            |
|                      | HER-2      | 2Rs15d                     | Breast Cancer (SKBR3), ovarian cancer (SKBR3)  | 70            |
|                      | MMR        | a-MMR                      | Mammary adenocarcinoma (TS/A), Lewis lung carcinoma (3LL-R)  | 37            |
|                      | CEA        | CEA1                       | Human colon adenocarcinoma (LS174)   | 72            |
|                      |            | NbCEA5 & humanized variant |  | 73            |
|                      | M-Protein  | R3B23                      | Multiple Myeloma (5T33MM)  | 75            |
|                      | Mesothelin | A1                         | Triple negative breast cancer (HCC70)  | 74            |
| Immune Checkpoint    | PDL-1      | C3, E2                     | PDL1 immune checkpoint   | 85            |
| Atherosclerosis      | LOX-1      | LOX-sdAb                   | Atherosclerosis (ApoE-deficient mice)  | 76            |
|                      | VCAM1      | cAbVCAM1-5                 |  | 65, 86–88     |
|                      | MMR        | a-MMR                      |  | 89            |
| Rheumatoid arthritis | MMR        | a-MMR                      | Rheumatoid arthritis   | 81            |
| Immune cells         | CR1g       | NbV4m119                   | Collagen-induced arthritis (CIA)   | 82            |
|                      | Unknown    | Nb-DC2.1                   | Myeloid cells  | 84            |
|                      |            | Nb-DC1.8                   | Immature bone marrow-derived dendritic cells   |               |
| Diabetes             | DPP6       | 4hD29                      |  | 77 and 78     |
| Liver disease        | Vsig4      | NbV4m119                   | Concanavalin A induced hepatitis   | 79            |
|                      | Clec4F     | C4m22                      | Concanavalin A induced hepatitis and methionine choline deficiency-induced non-alcoholic steatohepatitis | 80            |
|                      |            |                            |  | AGel mice     |

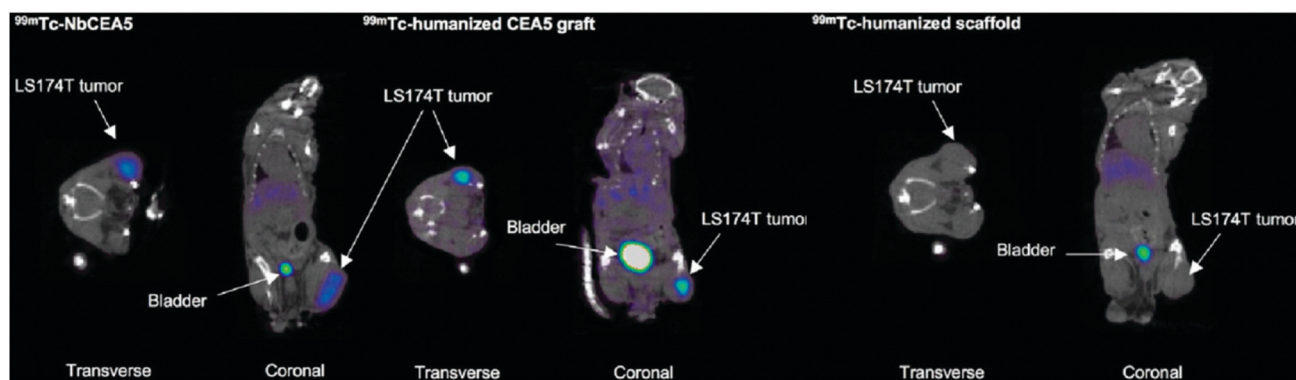


Fig. 5 SPECT imaging 1 h after injection of intravenously injected  $^{99m}\text{Tc}$ -labeled nanobodies. Both  $^{99m}\text{Tc}$ -NbCEA5 and  $^{99m}\text{Tc}$ -humanized CEA5 graft show high uptake in CEA-positive LS174T tumors in contrast to the  $^{99m}\text{Tc}$ -humanized scaffold alone. Adapted from ref. 73.

and intestines, tumor-specific uptake was above background (Fig. 6). In this clinical trial, Keyaerts *et al.* achieved safe, non-invasive visualization of HER2 status of both primary lesions and/or metastases. A phase II study of this tracer is underway (NCT03331601).

In addition to imaging the tumor's antigen profile, monitoring the immunological landscape in the TME could provide insight into the prognosis of a therapeutic response. Composition of the myeloid compartment, other immune cell types, cellular distribution and activation status could all be monitored. A nanobody against macrophage mannose receptor (MMR, CD206), a marker for M2-polarized macrophages the presence of which correlates with an immunosuppressive TME and poor prognosis, showed the presence of tumor-associated macrophages

(TAMs) in preclinical models.<sup>98,99</sup> A phase I clinical trial with  $^{68}\text{Ga}$ -NOTA-labeled anti-MMR nanobody is ongoing (NCT04168528). Nanobody-based PET tracers that target CD11b and major histocompatibility complex (MHC) class II positive cells, can track immune infiltrates in both xenogeneic and syngeneic tumor models.<sup>100</sup> In line with these findings, an anti-human MHC class II nanobody detects inflammation in a humanized graft-versus-host disease mouse model.<sup>101</sup>

The distribution of cytotoxic CD8+T cells could play a pivotal role in predicting the outcome of immune checkpoint blockade (ICB) therapy. Rashidian *et al.* demonstrated promising results in tracking CD8+T cell responses to ICB in preclinical models, using a  $^{89}\text{Zr}$ -labeled anti-CD8 nanobody.<sup>56,102</sup> Indeed, PET imaging showed a positive correlation between homogeneous



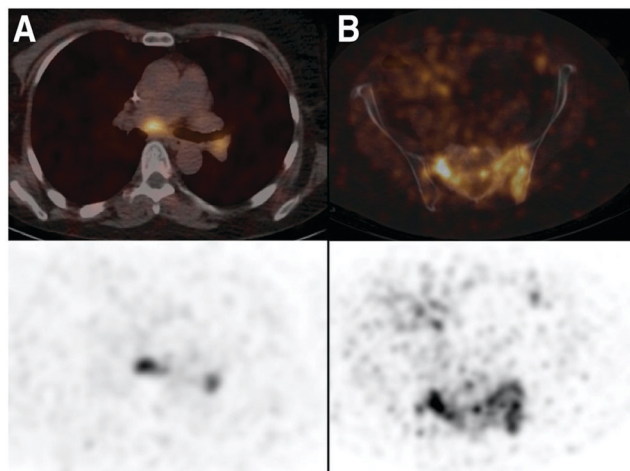


Fig. 6 PET/CT images from the phase I clinical trial of  $^{68}\text{Ga}$ -anti-HER2-Nanobody in breast cancer patients. (A) Patient 18, with invaded lymph nodes in the mediastinum and left hilar region. (B) Patient 20, with bone metastasis in the pelvis. PET/CT images (top) and PET images (bottom). Adapted from ref. 97.

distribution of CD8<sup>+</sup>T cells and responders to ICB therapy (Fig. 7). Similar to tracking of immune cells, non-invasive imaging of the targets of ICB may lead to better understanding of the intratumoral immunological landscape. Nanobody-based PET tracers against PD-L1 and CTLA-4, developed by Ingram *et al.*, showed distribution of checkpoint molecules in melanoma.<sup>103,104</sup> In yet another example, the extracellular

matrix (ECM) of tumors is a critical determinant for understanding the response to therapy. An anti-EIIIIB nanobody that recognizes an alternatively spliced variant of fibronectin in the ECM was developed and used for PET imaging of primary, metastatic and fibrotic lesions in preclinical cancer models.<sup>105</sup> An overview of some of the nanobody-based PET tracers is provided in Table 2.

#### 4.2. Infra-red imaging *in vivo*

Infra-red imaging is less sensitive than SPECT and PET. The amount of probe that must accumulate in the targeted area in order for it to be visible is much larger than that for SPECT and PET. Yet, recent development of fluorescent dyes in the infra-red and near infra-red region has led to the emergence of optical imaging as a viable technology for *in vivo* imaging.<sup>106–108</sup> IR/NIR imaging is flexible, sensitive, fast and relatively inexpensive compared to the radiolabeling approach for SPECT and PET, not to mention the advantage of avoiding radioactivity altogether.<sup>9</sup> Nanobodies conjugated to such dyes are now being used for *in vivo* imaging.<sup>23,48,109–112</sup> For example, Bannas *et al.* used a nanobody (s+16a) against the toxin-related ADP-ribosyltransferase ART2, an enzyme present on the surface of mouse T cells, to image lymph nodes in ART2-TG and ART2<sup>-/-</sup> mice using AlexaFluor 680.<sup>50</sup> For comparison, they also compared images of the cervical and axillary lymph nodes obtained with a nanobody-Fc fusion (s+16mFc) and the monoclonal antibody Nika102 (Fig. 8). Although all three constructs show *in vivo* fluorescence of the lymph nodes, s+16a shows no

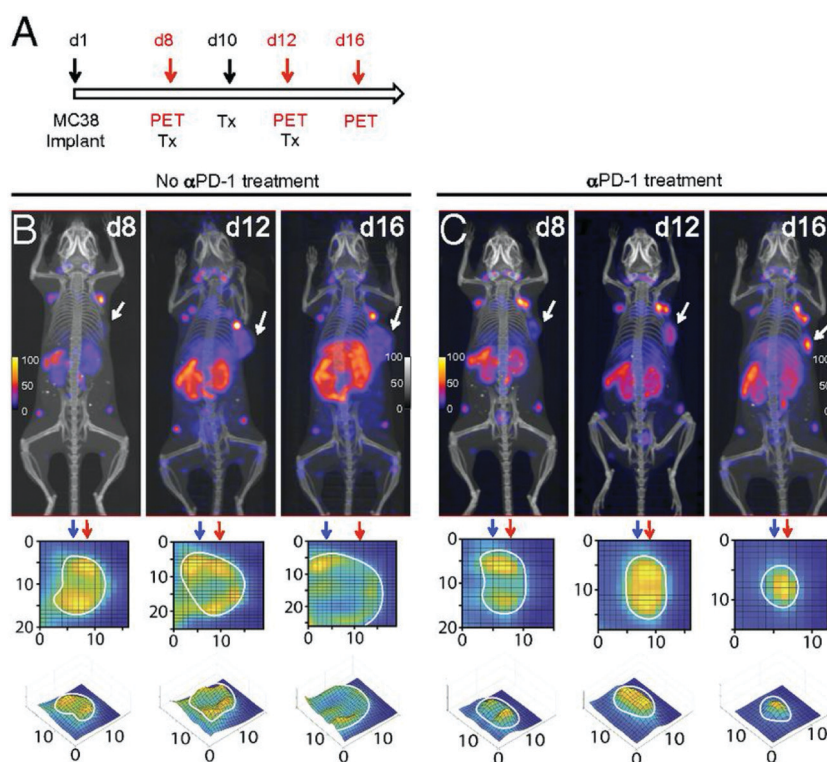


Fig. 7 Longitudinal monitoring of CD8<sup>+</sup> T cells in response to anti-PD-1 ( $\alpha$ PD-1) treatment. (A) Schematic for the treatment and PET imaging. (B and C) PET/CT images of tumor-bearing mice in the no treatment and treatment group. Adapted from ref. 102.





Table 2 Some nanobody-based tracers for non-invasive PET imaging

| Application          | Target           | Nanobody            | Disease model                                    | Ref           |
|----------------------|------------------|---------------------|--|---------------|
| Tumor biomarkers     | EGFR             | 7D12                | Skin cancer                                      | 34            |
|                      | HER2             | 2Rs15d 5F7          | Breast cancer                                    | 33, 93 and 94 |
|                      | HER3             | MSB0010853          | Non-small cell lung cancer, head and neck cancer | 57            |
|                      | CD20             | 9079                | Non-Hodgkin lymphoma                             | 95            |
|                      | HGF              | 1E6-Alb8, 6E10-Alb8 | Glioma   | 96            |
| Immune cells         | CD8              | VHH-X118            | Tumor immunology and inflammatory diseases       | 56 and 102    |
|                      | CD11b            | DC13                |  | 100           |
|                      | MHC II           | VHH7, VHH4          |  | 100 and 101   |
|                      | MMR              | MMR 3.49            |  | 98 and 99     |
| Checkpoint molecules | PD-L1            | B3                  | PD-L1 immune checkpoint                          | 103           |
|                      | CTLA-4           | H11                 | CTLA-4 immune checkpoint                         | 104           |
| ECM                  | Fibronectin EIIB | NJB2                | Breast cancer, PDAC, and melanoma                | 105           |



Fig. 8 Fast clearance of nanobodies allows rapid *in vivo* imaging after injection. ART2-TG mice and ART2<sup>-/-</sup> mice were injected with: buffer (control), 50 mg s+16a680, 5mg s+16mFc680 or 10 mg Nika102680. Control and antibody-injected mice (2 and 24 h after injection) were subjected to simultaneous imaging to obtain visually comparable images. Arrowheads indicate cervical and axillary lymph nodes. Adapted from ref. 50.

background signal, while strong background fluorescence was observed for Nika 102 and s+16mFc, particularly visible in the ART2<sup>-/-</sup> mice (Fig. 8).

Light scattering and light absorption by tissues limits the depth of penetration for NIR/IR imaging, ranging from microns to a few centimeters only.<sup>113,114</sup> Bleaching and blinking of fluorescent dyes also diminish the imaging signal strength over time. For these reasons, NIR/IR *in vivo* imaging is not suitable for whole-body imaging. Other systems that overcome these limitations are being developed and are being used for *in vivo* imaging. One such example is single-walled carbon nanotubes (SWCNTs). These nanomaterials present ideal optoelectronic characteristics for imaging in the IR region by emitting in the 850 to 1700 nm region.<sup>115</sup> This spectral window is highly

beneficial for biological and especially deep-tissue imaging, due to its reduced absorbance, phototoxicity, reduced background fluorescence and scattering as compared to traditional fluorescent dyes. SWCNTs do not bleach or blink, allowing longer exposure and imaging times. Mann *et al.* successfully used this type of imaging agent by conjugating it to a GFP-specific nanobody. To link SWCNTs to the nanobody a two-step process was deployed, using a maleimide-bearing oligonucleotide that wrapped itself around the SWCNT, followed by conjugation to the nanobody bearing a free cysteine residue. This construct was then used to monitor and track GFP-modified Kinesin-5 motor proteins in a *Drosophila* embryo (Fig. 9).<sup>116</sup>

One promising area where NIR/IR imaging may find application is in the context of intraoperative imaging to discriminate



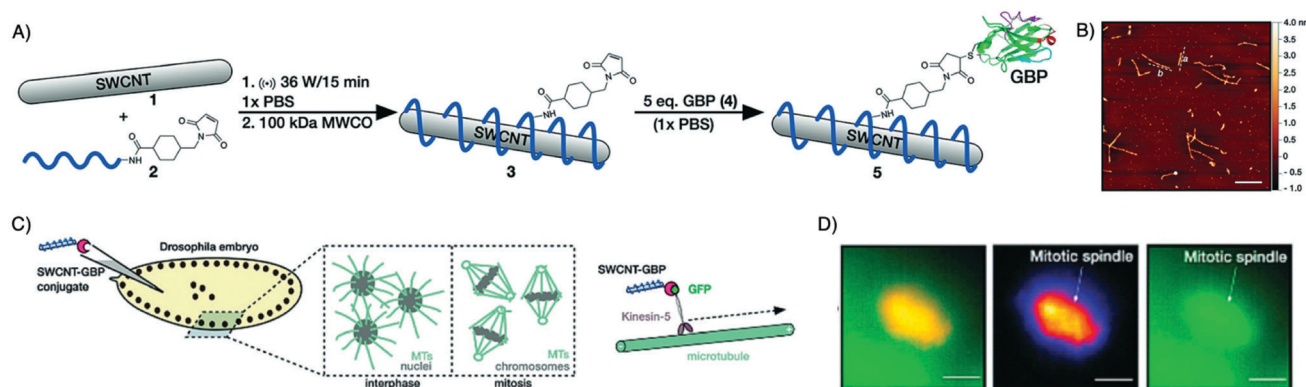


Fig. 9 Alternative to small molecule dyes for NIR/IR *in vivo* imaging. (A) Conjugation method for attaching a GFP-binding nanobody to DNA-wrapped SWCNTs. (B) Atomic force microscopy images of GBP-conjugated SWCNTs. Scale bar = 500 nm. (C) General scheme describing the injection of 5 into live *Drosophila* embryos expressing GFP proteins on Kin-5 motors. (D) GFP and SWCNT channel images showing colocalization of Kin-5 and conjugate 5 at a mitotic spindle (scale bars = 10 nm). Adapted from ref. 116.

malignant from healthy tissue and facilitate proper excision of a tumor.<sup>23</sup> This has dramatically improved surgery for removal of liver metastases, ovarian, cervical and breast cancer and melanoma.<sup>111</sup> Incomplete tissue penetration, which limits nanobody applications for whole body imaging, is less of a problem in this set-up. Indeed, nanobodies have been successfully used for such applications.<sup>23,48,110–112</sup>

Van Brussel *et al.* used a CAIX-specific nanobody, B9, modified *via* maleimide chemistry with a IRDye800CW dye. CAIX, carbonic anhydrase IX, is a tumor-specific membrane-bound protein expressed in hypoxic tumors.<sup>117,118</sup> Using a xenograft breast cancer mouse model of a ductal carcinoma *in situ* and mimicking a surgery set-up, strong accumulation of B9 was seen in the tumor, well differentiated from surrounding healthy tissue (Fig. 10A).<sup>110</sup>

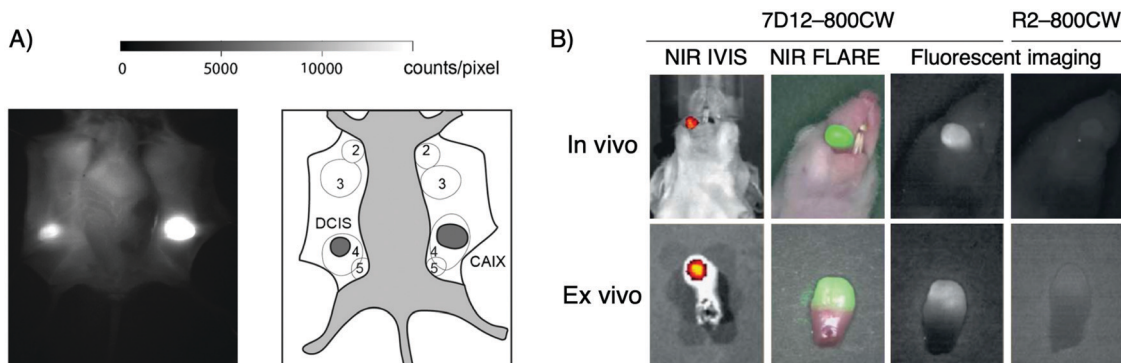


Fig. 10 Intraoperative imaging for cancer surgery. (A) Intra-operative imaging of DCIS and DCIS + CAIX tumors, 3 h post injection of fluorescently labeled VHH B9 (left). Schematic overview of mammary glands (2–5) and tumors as seen intra-operatively. DCIS + CAIX tumor indicated as “CAIX” in dark gray (right). (B) Real-time fluorescence imaging of orthotopic tongue tumor 24 hours after injection of the EGFR-specific nanobody 7D12 conjugated with IRDye800CW. Adapted from ref. 110.

Table 3 Overview of nanobody-based tracers for non-invasive IR/NIR imaging and intraoperative imaging

| Target    | Nanobody | Fluorescent Dye                        | Disease model  | Ref                     |
|-----------|----------|--|--|-------------------------|
| EGFR      | 7D12     | IRDye800CW                             | Human epidermoid carcinoma (A431)  | 36                      |
| HER-2     | 11A4     | IRDye800CW                             | Breast cancer (SKBR3),<br>Breast cancer (MCF10DCIS)                          | 38<br>30                |
|           | 2Rs15d   | IRDye680RD<br>IRDye800CW<br>IRDye680RD | Breast cancer (SKOV3)  | 109<br>49 and 112<br>49 |
| CAIX      | B9       | Cy5<br>IRDye800CW                      | Breast cancer (BT474M1)<br>Breast cancer (MCF10DCIS)<br>Breast cancer (DCIS) | 119<br>109<br>110       |
| ART2      | s+16a    | AlexaFluor 680                         | ART2-TG  | 50                      |
| CEA       | Anti-CEA | IRDye800CW                             | Human pancreatic cancer (BxPC-3 and MiaPACA-2)                               | 120                     |
| Kin-5-GFP | GBP      | SWCNT                                  | GFP fusion proteins of Kin-5 motors  | 116                     |



Another example reported by van Driel *et al.* used a nanobody that targets EGFR, 7D12, conjugated to IRDye800CW for the imaging of a tongue tumor (Fig. 10B). Not only were they able to clearly identify the primary tumor, the imaging agent also detected cervical lymph node metastases.<sup>48</sup>

Although NIR/IR *in vivo* imaging might not be as sensitive as the radiolabeling methods, it represents an appealing alternative, especially in the case of intraoperative imaging for cancer surgery. A summary of the different nanobodies used for NIR/IR *in vivo* imaging and for intraoperative imaging is shown in Table 3.

## 5. Conclusions

Here we reviewed recent advances in the field of molecular imaging using nanobody-based probes. The unique properties of nanobodies make them ideal targeting agents, and not just for *in vivo* imaging. Their rapid clearance from the circulation, their tissue penetration properties, and their low background retention enable highly specific imaging at early time points after administration, even on the same day, with a reduced risk of nonspecific toxicity. Unfortunately, this advantage over the regular antibodies leads generally to an important kidney uptake. However, methods, such as PEGylation, are emerging to overcome this challenge. Although most of the applications reported to date using nanobodies have employed SPECT or PET as the imaging modality, other techniques such as infrared imaging, especially in the case of intraoperative surgery, ultrasound,<sup>121–123</sup> photoacoustic imaging,<sup>124,125</sup> and Magnetic Resonance Imaging (MRI)<sup>126–128</sup> deserve attention.

The results obtained to date with nanobodies for molecular imaging show that these tracers will find many applications in the laboratory as well as in the clinic. The preclinical success of nanobodies justifies further exploration and development to expand molecular imaging, ultimately with a view to clinical success.

## Conflicts of interest

There are no conflicts to declare.

## Acknowledgements

This work was supported by NIH Grants 1R01CA255216-01. A. I. was supported by the Norwegian Cancer Society (Project no. 198164) and the overseas grant from UiT The Arctic University of Norway. N.P. was supported by the Society of Fellows, Harvard University.

## References

- 1 R. Weissleder and M. J. Pittet, Imaging in the Era of Molecular Oncology, *Nature*, 2008, **452**(7187), 580–589, DOI: 10.1038/nature06917.

- 2 Y. Wu, W. Zhang, J. Li and Y. Zhang, Optical Imaging of Tumor Microenvironment. *Am, J. Nucl. Med. Mol. Imaging*, 2013, **3**(1), 1–15.
- 3 J. M. Hoffman and S. S. Gambhir, Molecular Imaging: The Vision and Opportunity for Radiology in the Future, *Radiology*, 2007, **244**(1), 39–47, DOI: 10.1148/radiol.2441060773.
- 4 S. S. Gambhir, Molecular Imaging of Cancer with Positron Emission Tomography, *Nat. Rev. Cancer*, 2002, **2**(9), 683–693, DOI: 10.1038/nrc882.
- 5 P. J. Cassidy and G. K. Radda, Molecular Imaging Perspectives, *J. R. Soc., Interface*, 2005, **2**(3), 133–144, DOI: 10.1098/rsif.2005.0040.
- 6 H. R. Herschman, Molecular Imaging: Looking at Problems, Seeing Solutions, *Science*, 2003, **302**(5645), 605–608, DOI: 10.1126/science.1090585.
- 7 T. F. Massoud and S. S. Gambhir, Molecular Imaging in Living Subjects: Seeing Fundamental Biological Processes in a New Light, *Genes Dev.*, 2003, **17**(5), 545–580, DOI: 10.1101/gad.1047403.
- 8 B. J. Pichler, H. F. Wehrl and M. S. Judenhofer, Latest Advances in Molecular Imaging Instrumentation, *J. Nucl. Med. Off. Publ. Soc. Nucl. Med.*, 2008, **49**(Suppl 2), 5S–23S, DOI: 10.2967/jnumed.108.045880.
- 9 R. Chakravarty, S. Goel and W. Cai, Nanobody: The “Magic Bullet” for Molecular Imaging?, *Theranostics*, 2014, **4**(4), 386–398, DOI: 10.7150/thno.8006.
- 10 A. M. Wu, Engineered Antibodies for Molecular Imaging of Cancer, *Methods San Diego Calif*, 2014, **65**(1), 139–147, DOI: 10.1016/j.ymeth.2013.09.015.
- 11 J. C. Reubi and H. R. Maecke, Peptide-Based Probes for Cancer Imaging, *J. Nucl. Med. Off. Publ. Soc. Nucl. Med.*, 2008, **49**(11), 1735–1738, DOI: 10.2967/jnumed.108.053041.
- 12 L. Zhu, N. Guo, Q. Li, Y. Ma, O. Jacobson, S. Lee, H. S. Choi, J. R. Mansfield, G. Niu and X. Chen, Dynamic PET and Optical Imaging and Compartment Modeling Using a Dual-Labeled Cyclic RGD Peptide Probe, *Theranostics*, 2012, **2**(8), 746–756, DOI: 10.7150/thno.4762.
- 13 M. Cui, Past and Recent Progress of Molecular Imaging Probes for  $\beta$ -Amyloid Plaques in the Brain, *Curr. Med. Chem.*, 2014, **21**(1), 82–112, DOI: 10.2174/09298673113209990216.
- 14 B. Kim, J. Yang, M. Hwang, J. Choi, H.-O. Kim, E. Jang, J. H. Lee, S.-H. Ryu, J.-S. Suh, Y.-M. Huh and S. Haam, Aptamer-Modified Magnetic Nanoprobe for Molecular MR Imaging of VEGFR2 on Angiogenic Vasculature, *Nanoscale Res. Lett.*, 2013, **8**(1), 399, DOI: 10.1186/1556-276X-8-399.
- 15 K. Varmira, S. J. Hosseinimehr, Z. Noaparast and S. M. Abedi, An Improved Radiolabelled RNA Aptamer Molecule for HER2 Imaging in Cancers, *J. Drug Target.*, 2014, **22**(2), 116–122, DOI: 10.3109/1061186X.2013.839688.
- 16 A. C. Freise and A. M. Wu, In Vivo Imaging with Antibodies and Engineered Fragments, *Mol. Immunol.*, 2015, **67**(2 Pt A), 142–152, DOI: 10.1016/j.molimm.2015.04.001.
- 17 T. Romer, H. Leonhardt and U. Rothbauer, Engineering Antibodies and Proteins for Molecular *in Vivo* Imaging,





- Curr. Opin. Biotechnol.*, 2011, 22(6), 882–887, DOI: 10.1016/j.copbio.2011.06.007.
- 18 M. Morais and M. T. Ma, Site-Specific Chelator-Antibody Conjugation for PET and SPECT Imaging with Radiometals, *Drug Discovery Today Technol.*, 2018, 30, 91–104, DOI: 10.1016/j.ddtec.2018.10.002.
- 19 D. Smolarek, O. Bertrand and M. Czerwinski, Variable Fragments of Heavy Chain Antibodies (VHHs): A New Magic Bullet Molecule of Medicine?, *Postepy Hig. Med. Doswiadczalnej Online*, 2012, 66, 348–358, DOI: 10.5604/17322693.1000334.
- 20 T. Olafsen and A. M. Wu, Antibody Vectors for Imaging, *Semin. Nucl. Med.*, 2010, 40(3), 167–181, DOI: 10.1053/j.semnuclmed.2009.12.005.
- 21 S. Kaur, G. Venktaraman, M. Jain, S. Senapati, P. K. Garg and S. K. Batra, Recent Trends in Antibody-Based Oncologic Imaging, *Cancer Lett.*, 2012, 315(2), 97–111, DOI: 10.1016/j.canlet.2011.10.017.
- 22 P. Holliger and P. J. Hudson, Engineered Antibody Fragments and the Rise of Single Domains, *Nat. Biotechnol.*, 2005, 23(9), 1126–1136, DOI: 10.1038/nbt1142.
- 23 P. Debie, N. Devoogdt and S. Hernot, Targeted Nanobody-Based Molecular Tracers for Nuclear Imaging and Image-Guided Surgery, *Antibodies Basel Switz.*, 2019, 8, 12, DOI: 10.3390/antib8010012.
- 24 R. W. Cheloha, T. J. Harmand, C. Wijne, T. U. Schwartz and H. L. Ploegh, Exploring Cellular Biochemistry with Nanobodies, *J. Biol. Chem.*, 2020, 295(45), 15307–15327, DOI: 10.1074/jbc.REV120.012960.
- 25 G. Hassanzadeh-Ghassabeh, N. Devoogdt, P. De Pauw, C. Vincke and S. Muyldermans, Nanobodies and Their Potential Applications, *Nanomed.*, 2013, 8(6), 1013–1026, DOI: 10.2217/nnm.13.86.
- 26 I. Beltrán Hernández, R. Rompen, R. Rossin, K. T. Xenaki, E. A. Katrukha, K. Nicolay, P. van Bergen En Henegouwen, H. Grüll and S. Oliveira, Imaging of Tumor Spheroids, Dual-Isotope SPECT, and Autoradiographic Analysis to Assess the Tumor Uptake and Distribution of Different Nanobodies, *Mol. Imaging Biol.*, 2019, 21(6), 1079–1088, DOI: 10.1007/s11307-019-01320-x.
- 27 P. Debie, C. Lafont, M. Defrise, I. Hansen, D. M. van Willigen, F. W. B. van Leeuwen, R. Gijssbers, M. D'Huyvetter, N. Devoogdt, T. Lahoutte, P. Mollard and S. Hernot, Size and Affinity Kinetics of Nanobodies Influence Targeting and Penetration of Solid Tumours, *J. Control. Release Off. J. Control. Release Soc.*, 2020, 317, 34–42, DOI: 10.1016/j.jconrel.2019.11.014.
- 28 I. Vaneycken, M. D'huyvetter, S. Hernot, J. De Vos, C. Xavier, N. Devoogdt, V. Caveliers and T. Lahoutte, Immuno-Imaging Using Nanobodies, *Curr. Opin. Biotechnol.*, 2011, 22(6), 877–881, DOI: 10.1016/j.copbio.2011.06.009.
- 29 C. Vincke, R. Loris, D. Saerens, S. Martinez-Rodriguez, S. Muyldermans and K. Conrath, General Strategy to Humanize a Camelid Single-Domain Antibody and Identification of a Universal Humanized Nanobody Scaffold, *J. Biol. Chem.*, 2009, 284(5), 3273–3284, DOI: 10.1074/jbc.M806889200.
- 30 R. C. Ladenson, D. L. Crimmins, Y. Landt and J. H. Ladenson, Isolation and Characterization of a Thermally Stable Recombinant Anti-Caffeine Heavy-Chain Antibody Fragment, *Anal. Chem.*, 2006, 78(13), 4501–4508, DOI: 10.1021/ac058044j.
- 31 L. O. T. Gainkam, V. Caveliers, N. Devoogdt, C. Vanhove, C. Xavier, O. Boerman, S. Muyldermans, A. Bossuyt and T. Lahoutte, Localization, Mechanism and Reduction of Renal Retention of Technetium-99m Labeled Epidermal Growth Factor Receptor-Specific Nanobody in Mice, *Contrast Media Mol. Imaging*, 2011, 6(2), 85–92, DOI: 10.1002/cmml.408.
- 32 L. Huang, L. O. T. Gainkam, V. Caveliers, C. Vanhove, M. Keyaerts, P. De Baetselier, A. Bossuyt, H. Revets and T. Lahoutte, SPECT Imaging with 99mTc-Labeled EGFR-Specific Nanobody for in Vivo Monitoring of EGFR Expression, *Mol. Imaging Biol.*, 2008, 10(3), 167–175, DOI: 10.1007/s11307-008-0133-8.
- 33 C. Xavier, I. Vaneycken, M. D'huyvetter, J. Heemskerk, M. Keyaerts, C. Vincke, N. Devoogdt, S. Muyldermans, T. Lahoutte and V. Caveliers, Synthesis, Preclinical Validation, Dosimetry, and Toxicity of 68Ga-NOTA-Anti-HER2 Nanobodies for IPET Imaging of HER2 Receptor Expression in Cancer, *J. Nucl. Med. Off. Publ. Soc. Nucl. Med.*, 2013, 54(5), 776–784, DOI: 10.2967/jnumed.112.111021.
- 34 M. J. W. D. Vosjan, L. R. Perk, R. C. Roovers, G. W. M. Visser, M. Stigter-van Walsum, P. M. P. van Bergen En Henegouwen and G. A. M. S. van Dongen, Facile Labelling of an Anti-Epidermal Growth Factor Receptor Nanobody with 68Ga via a Novel Bifunctional Desferal Chelate for Immuno-PET, *Eur. J. Nucl. Med. Mol. Imaging*, 2011, 38(4), 753–763, DOI: 10.1007/s00259-010-1700-1.
- 35 S. Oliveira, R. Heukers, J. Sornkom, R. J. Kok and P. M. P. van Bergen En Henegouwen, Targeting Tumors with Nanobodies for Cancer Imaging and Therapy, *J. Control. Release Off. J. Control. Release Soc.*, 2013, 172(3), 607–617, DOI: 10.1016/j.jconrel.2013.08.298.
- 36 S. Oliveira, G. A. M. S. van Dongen, M. Stigter-van Walsum, R. C. Roovers, J. C. Stam, W. Mali, P. J. van Diest and P. M. P. van Bergen en Henegouwen, Rapid Visualization of Human Tumor Xenografts through Optical Imaging with a Near-Infrared Fluorescent Anti-Epidermal Growth Factor Receptor Nanobody, *Mol. Imaging*, 2012, 11(1), 33–46.
- 37 K. Movahedi, S. Schoonoghe, D. Laoui, I. Houbracken, W. Waelput, K. Breckpot, L. Bouwens, T. Lahoutte, P. De Baetselier, G. Raes, N. Devoogdt and J. A. Van Ginderachter, Nanobody-Based Targeting of the Macrophage Mannose Receptor for Effective in Vivo Imaging of Tumor-Associated Macrophages, *Cancer Res.*, 2012, 72(16), 4165–4177, DOI: 10.1158/0008-5472.CAN-11-2994.
- 38 M. Kijanka, F.-J. Warnders, M. El Khattabi, M. Lub-de Hooge, G. M. van Dam, V. Ntziachristos, L. de Vries, S. Oliveira and P. M. P. van Bergen En Henegouwen, Rapid Optical Imaging of Human Breast Tumour Xenografts Using Anti-HER2 VHHs Site-Directly Conjugated to IRDye



- 800CW for Image-Guided Surgery, *Eur. J. Nucl. Med. Mol. Imaging*, 2013, **40**(11), 1718–1729, DOI: 10.1007/s00259-013-2471-2.
- 39 A. Badar, J. Williams, R. T. de Rosales, R. Tavaré, F. Kampmeier, P. J. Blower and G. E. Mullen, Optimising the Radiolabelling Properties of Technetium Tricarbonyl and His-Tagged Proteins, *EJNMMI Res*, 2014, **4**(1), 14, DOI: 10.1186/2191-219X-4-14.
- 40 R. Waibel, R. Alberto, J. Willuda, R. Finnern, R. Schibli, A. Stichelberger, A. Egli, U. Abram, J. P. Mach, A. Plückthun and P. A. Schubiger, Stable One-Step Technetium-99m Labeling of His-Tagged Recombinant Proteins with a Novel Tc(I)-Carbonyl Complex, *Nat. Biotechnol.*, 1999, **17**(9), 897–901, DOI: 10.1038/12890.
- 41 S. Massa, C. Xavier, S. Muyldermans and N. Devoogdt, Emerging Site-Specific Bioconjugation Strategies for Radioimmunotracer Development, *Expert Opin. Drug Delivery*, 2016, **13**(8), 1149–1163, DOI: 10.1080/17425247.2016.1178235.
- 42 D. Schumacher, J. Helma, A. F. L. Schneider, H. Leonhardt and C. P. R. Hackenberger, Nanobodies: Chemical Functionalization Strategies and Intracellular Applications, *Angew. Chem., Int. Ed.*, 2018, **57**(9), 2314–2333, DOI: 10.1002/anie.201708459.
- 43 M. J. Adam and D. S. Wilbur, Radiohalogens for Imaging and Therapy, *Chem. Soc. Rev.*, 2005, **34**(2), 153–163, DOI: 10.1039/b313872k.
- 44 H. S. Krishnan, L. Ma, N. Vasdev and S. H. Liang, 18 F-Labeling of Sensitive Biomolecules for Positron Emission Tomography, *Chem. Weinh. Bergstr. Ger.*, 2017, **23**(62), 15553–15577, DOI: 10.1002/chem.201701581.
- 45 P. P. Ghoroghchian, M. J. Therien and D. A. Hammer, *In Vivo* Fluorescence Imaging: A Personal Perspective, *Wiley Interdiscip. Rev. Nanomed. Nanobiotechnol.*, 2009, **1**(2), 156–167, DOI: 10.1002/wnan.7.
- 46 X. Zhang, S. Bloch, W. Akers and S. Achilefu, Near-Infrared Molecular Probes for *in Vivo* Imaging, *Curr. Protoc. Cytom.*, 2012, **ch 12**, Unit 12.27, DOI: 10.1002/0471142956.cy1227s60.
- 47 G. M. Fischer, M. Isomäki-Krondahl, I. Göttker-Schnetmann, E. Daltrozzo and A. Zumbusch, Pyrrolopyrrole Cyanine Dyes: A New Class of near-Infrared Dyes and Fluorophores, *Chem. Weinh. Bergstr. Ger.*, 2009, **15**(19), 4857–4864, DOI: 10.1002/chem.200801996.
- 48 P. B. a. A. van Driel, J. R. van der Vorst, F. P. R. Verbeek, S. Oliveira, T. J. A. Snoeks, S. Keereweer, B. Chan, M. C. Boonstra, J. V. Frangioni, P. M. P. van Bergen en Henegouwen, A. L. Vahrmeijer and C. W. G. M. Lowik, Intraoperative Fluorescence Delineation of Head and Neck Cancer with a Fluorescent Anti-Epidermal Growth Factor Receptor Nanobody, *Int. J. Cancer*, 2014, **134**(11), 2663–2673, DOI: 10.1002/ijc.28601.
- 49 P. Debie, J. Van Quathem, I. Hansen, G. Bala, S. Massa, N. Devoogdt, C. Xavier and S. Hernot, Effect of Dye and Conjugation Chemistry on the Biodistribution Profile of Near-Infrared-Labeled Nanobodies as Tracers for Image-Guided Surgery, *Mol. Pharm.*, 2017, **14**(4), 1145–1153, DOI: 10.1021/acs.molpharmaceut.6b01053.
- 50 P. Bannas, L. Well, A. Lenz, B. Rissiek, F. Haag, J. Schmid, K. Hochgräfe, M. Trepel, G. Adam, H. Ittrich and F. Koch-Nolte, *In Vivo* Near-Infrared Fluorescence Targeting of T Cells: Comparison of Nanobodies and Conventional Monoclonal Antibodies, *Contrast Media Mol. Imaging*, 2014, **9**(2), 135–142, DOI: 10.1002/cmimi.1548.
- 51 P. Bannas, A. Lenz, V. Kunick, L. Well, W. Fumey, B. Rissiek, F. Haag, J. Schmid, K. Schütze, A. Eichhoff, M. Trepel, G. Adam, H. Ittrich and F. Koch-Nolte, Molecular Imaging of Tumors with Nanobodies and Antibodies: Timing and Dosage Are Crucial Factors for Improved *In Vivo* Detection, *Contrast Media Mol. Imaging*, 2015, **10**(5), 367–378, DOI: 10.1002/cmimi.1637.
- 52 T. M. Behr, R. M. Sharkey, M. E. Juweid, R. D. Blumenthal, R. M. Dunn, G. L. Griffiths, H. J. Bair, F. G. Wolf, W. S. Becker and D. M. Goldenberg, Reduction of the Renal Uptake of Radiolabeled Monoclonal Antibody Fragments by Cationic Amino Acids and Their Derivatives, *Cancer Res.*, 1995, **55**(17), 3825–3834.
- 53 M. de Jong, R. Barone, E. Krenning, B. Bernard, M. Melis, T. Visser, M. Gekele, T. E. Willnow, S. Walrand, F. Jamar and S. Pauwels, Megalin Is Essential for Renal Proximal Tubule Reabsorption of (111)In-DTPA-Octreotide, *J. Nucl. Med. Off. Publ. Soc. Nucl. Med.*, 2005, **46**(10), 1696–1700.
- 54 K. L. S. Chatalic, J. Veldhoven-Zweistra, M. Bolkestein, S. Hoeben, G. A. Koning, O. C. Boerman, M. de Jong and W. M. van Weerden, A Novel <sup>111</sup>In-Labeled Anti-Prostate-Specific Membrane Antigen Nanobody for Targeted SPECT/CT Imaging of Prostate Cancer, *J. Nucl. Med. Off. Publ. Soc. Nucl. Med.*, 2015, **56**(7), 1094–1099, DOI: 10.2967/jnumed.115.156729.
- 55 M. D'Huyvetter, C. Vincke, C. Xavier, A. Aerts, N. Impens, S. Baatout, H. De Raeve, S. Muyldermans, V. Cavelliers, N. Devoogdt and T. Lahoutte, Targeted Radionuclide Therapy with A 177Lu-Labeled Anti-HER2 Nanobody, *Theranostics*, 2014, **4**(7), 708–720, DOI: 10.7150/thno.8156.
- 56 M. Rashidian, J. R. Ingram, M. Dougan, A. Dongre, K. A. Whang, C. LeGall, J. J. Cragolini, B. Bieri, M. Gostissa, J. Gorman, G. M. Grotenbreg, A. Bhan, R. A. Weinberg and H. L. Ploegh, Predicting the Response to CTLA-4 Blockade by Longitudinal Noninvasive Monitoring of CD8 T Cells, *J. Exp. Med.*, 2017, **214**(8), 2243–2255, DOI: 10.1084/jem.20161950.
- 57 F. J. Warnders, A. G. T. Terwisscha van Scheltinga, C. Knuehl, M. van Roy, E. F. J. de Vries, J. G. W. Kosterink, E. G. E. de Vries and M. N. Lub-de Hooge, Human Epidermal Growth Factor Receptor 3-Specific Tumor Uptake and Biodistribution of 89Zr-MSB0010853 Visualized by Real-Time and Noninvasive PET Imaging, *J. Nucl. Med. Off. Publ. Soc. Nucl. Med.*, 2017, **58**(8), 1210–1215, DOI: 10.2967/jnumed.116.181586.
- 58 C. M. Gomes, A. J. Abrunhosa, P. Ramos and E. K. J. Pauwels, Molecular Imaging with SPECT as a Tool for Drug Development, *Adv. Drug Delivery Rev.*, 2011, **63**(7), 547–554, DOI: 10.1016/j.addr.2010.09.015.



- 59 S. M. Ametamey, M. Honer and P. A. Schubiger, Molecular Imaging with PET, *Chem. Rev.*, 2008, **108**(5), 1501–1516, DOI: 10.1021/cr0782426.
- 60 T. Van den Wyngaert, F. Elvas, S. De Schepper, J. A. Kennedy and O. Israel, SPECT/CT: Standing on the Shoulders of Giants, It Is Time to Reach for the Sky!, *J. Nucl. Med. Off. Publ. Soc. Nucl. Med.*, 2020, **61**(9), 1284–1291, DOI: 10.2967/jnumed.119.236943.
- 61 V. Filippou and C. Tsoumpas, Recent Advances on the Development of Phantoms Using 3D Printing for Imaging with CT, MRI, PET, SPECT, and Ultrasound, *Med. Phys.*, 2018, **45**(9), e740–e760.
- 62 E. Piekarski, A. Manrique, F. Rouzet and D. Le Guludec, Current Status of Myocardial Perfusion Imaging With New SPECT/CT Cameras, *Semin. Nucl. Med.*, 2020, **50**(3), 219–226, DOI: 10.1053/j.semnuclmed.2020.02.009.
- 63 J. Wu and C. Liu, Recent Advances in Cardiac SPECT Instrumentation and Imaging Methods, *Phys. Med. Biol.*, 2019, **64**(6), 06TR01, DOI: 10.1088/1361-6560/ab04de.
- 64 C. Müller, E. Fischer, M. Behe, U. Köster, H. Dorrer, J. Reber, S. Haller, S. Cohrs, A. Blanc, J. Grünberg, M. Bunka, K. Zhernosekov, N. van der Meulen, K. Johnston, A. Türler and R. Schibli, Future Prospects for SPECT Imaging Using the Radiolanthanide Terbium-155 – Production and Preclinical Evaluation in Tumor-Bearing Mice, *Nucl. Med. Biol.*, 2014, **41**, e58–e65, DOI: 10.1016/j.nucmedbio.2013.11.002.
- 65 G. Bala, M. Crauwels, A. Blykers, I. Remory, A. L. J. Marschall, S. Dübel, L. Dumas, A. Broisat, C. Martin, S. Ballet, B. Cosyns, V. Caveliers, N. Devoogdt, C. Xavier and S. Hernot, Radiometal-Labeled Anti-VCAM-1 Nanobodies as Molecular Tracers for Atherosclerosis - Impact of Radiochemistry on Pharmacokinetics, *Biol. Chem.*, 2019, **400**(3), 323–332, DOI: 10.1515/hsz-2018-0330.
- 66 T. Krüwel, D. Nevoltris, J. Bode, C. Dullin, D. Baty, P. Chames and F. Alves, In Vivo Detection of Small Tumour Lesions by Multi-Pinhole SPECT Applying a (99m)Tc-Labelled Nanobody Targeting the Epidermal Growth Factor Receptor, *Sci. Rep.*, 2016, **6**, 21834, DOI: 10.1038/srep21834.
- 67 W. C. Eckelman, Unparalleled Contribution of Technetium-99m to Medicine over 5 Decades, *JACC Cardiovasc. Imaging*, 2009, **2**(3), 364–368, DOI: 10.1016/j.jcmg.2008.12.013.
- 68 L. O. T. Gainkam, L. Huang, V. Caveliers, M. Keyaerts, S. Hernot, I. Vaneycken, C. Vanhove, H. Revets, P. De Baetselier and T. Lahoutte, Comparison of the Biodistribution and Tumor Targeting of Two 99mTc-Labeled Anti-EGFR Nanobodies in Mice, Using Pinhole SPECT/Micro-CT, *J. Nucl. Med. Off. Publ. Soc. Nucl. Med.*, 2008, **49**(5), 788–795, DOI: 10.2967/jnumed.107.048538.
- 69 L. O. T. Gainkam, M. Keyaerts, V. Caveliers, N. Devoogdt, C. Vanhove, L. Van Grunsven, S. Muyltermans and T. Lahoutte, Correlation between Epidermal Growth Factor Receptor-Specific Nanobody Uptake and Tumor Burden: A Tool for Noninvasive Monitoring of Tumor Response to Therapy, *Mol. Imaging Biol.*, 2011, **13**(5), 940–948, DOI: 10.1007/s11307-010-0428-4.
- 70 I. Vaneycken, N. Devoogdt, N. Van Gassen, C. Vincke, C. Xavier, U. Wernery, S. Muyltermans, T. Lahoutte and V. Caveliers, Preclinical Screening of Anti-HER2 Nanobodies for Molecular Imaging of Breast Cancer, *FASEB J. Off. Publ. Fed. Am. Soc. Exp. Biol.*, 2011, **25**(7), 2433–2446, DOI: 10.1096/fj.10-180331.
- 71 M. Evazalipour, M. D'Huyvetter, B. S. Tehrani, M. Abolhassani, K. Omidfar, S. Abdoli, R. Arezumand, H. Morowati, T. Lahoutte, S. Muyltermans and N. Devoogdt, Generation and Characterization of Nanobodies Targeting PSMA for Molecular Imaging of Prostate Cancer, *Contrast Media Mol. Imaging*, 2014, **9**(3), 211–220, DOI: 10.1002/cmml.1558.
- 72 V. Caveliers, V. Cortez-Retamozo, T. Lahoutte, L. Tchouate Gainkam, S. Hernot, A. Packeu, F. Vos, C. Vanhove, S. Muyltermans, P. Baetselier and H. Revets, 99mTc-Labeled Nanobodies: A New Type of Targeted Probes for Imaging Antigen Expression, *Curr. Radiopharm.*, 2008, **1**(1), 37–41, DOI: 10.2174/1874471010801010037.
- 73 I. Vaneycken, J. Govaert, C. Vincke, V. Caveliers, T. Lahoutte, P. De Baetselier, G. Raes, A. Bossuyt, S. Muyltermans and N. Devoogdt, In Vitro Analysis and in Vivo Tumor Targeting of a Humanized, Grafted Nanobody in Mice Using Pinhole SPECT/Micro-CT, *J. Nucl. Med. Off. Publ. Soc. Nucl. Med.*, 2010, **51**(7), 1099–1106, DOI: 10.2967/jnumed.109.069823.
- 74 C. Montemagno, S. Bacot, M. Ahmadi, B. Kerfelec, D. Baty, M. Debiossat, A. Soubies, P. Perret, L. Riou, D. Fagret, A. Broisat and C. Ghezzi, Preclinical Evaluation of Mesothelin-Specific Ligands for SPECT Imaging of Triple-Negative Breast Cancer, *J. Nucl. Med. Off. Publ. Soc. Nucl. Med.*, 2018, **59**(7), 1056–1062, DOI: 10.2967/jnumed.117.203489.
- 75 M. Lemaire, M. D'Huyvetter, T. Lahoutte, E. Van Valckenborgh, E. Menu, E. De Bruyne, P. Kronenberger, U. Wernery, S. Muyltermans, N. Devoogdt and K. Vanderkerken, Imaging and Radioimmunotherapy of Multiple Myeloma with Anti-Idiotypic Nanobodies, *Leukemia*, 2014, **28**(2), 444–447, DOI: 10.1038/leu.2013.292.
- 76 J. De Vos, I. Mathijs, C. Xavier, S. Massa, U. Wernery, L. Bouwens, T. Lahoutte, S. Muyltermans and N. Devoogdt, Specific Targeting of Atherosclerotic Plaques in ApoE(–/–) Mice Using a New Camelid SdAb Binding the Vulnerable Plaque Marker LOX-1, *Mol. Imaging Biol.*, 2014, **16**(5), 690–698, DOI: 10.1007/s11307-014-0731-6.
- 77 S. Demine, R. Garcia Ribeiro, J. Thevenet, L. Marselli, P. Marchetti, F. Pattou, J. Kerr-Conte, N. Devoogdt and D. L. Eizirik, A Nanobody-Based Nuclear Imaging Tracer Targeting Dipeptidyl Peptidase 6 to Determine the Mass of Human Beta Cell Grafts in Mice, *Diabetologia*, 2020, **63**(4), 825–836, DOI: 10.1007/s00125-019-05068-5.
- 78 A. Balhuizen, S. Massa, I. Mathijs, J.-V. Turatsinze, J. De Vos, S. Demine, C. Xavier, O. Villate, I. Millard, D. Egrise, C. Capito, R. Scharfmann, P. In't Veld, P. Marchetti, S. Muyltermans, S. Goldman, T. Lahoutte, L. Bouwens, D. L. Eizirik and N. Devoogdt, A Nanobody-Based Tracer





- Targeting DPP6 for Non-Invasive Imaging of Human Pancreatic Endocrine Cells, *Sci. Rep.*, 2017, 7(1), 15130, DOI: 10.1038/s41598-017-15417-2.
- 79 F. Zheng, N. Devoogdt, A. Sparkes, Y. Morias, C. Abels, B. Stijlemans, T. Lahoutte, S. Muyltermans, P. De Baetselier, S. Schoonooghe, A. Beschin and G. Raes, Monitoring Liver Macrophages Using Nanobodies Targeting Vsig4: Concanavalin A Induced Acute Hepatitis as Paradigm, *Immunobiology*, 2015, 220(2), 200–209, DOI: 10.1016/j.imbio.2014.09.018.
- 80 F. Zheng, A. Sparkes, P. De Baetselier, S. Schoonooghe, B. Stijlemans, S. Muyltermans, V. Flamand, J. A. Van Ginderachter, N. Devoogdt, G. Raes and A. Beschin, Molecular Imaging with Kupffer Cell-Targeting Nanobodies for Diagnosis and Prognosis in Mouse Models of Liver Pathogenesis, *Mol. Imaging Biol.*, 2017, 19(1), 49–58, DOI: 10.1007/s11307-016-0976-3.
- 81 S. Put, S. Schoonooghe, N. Devoogdt, E. Schurgers, A. Avau, T. Mitera, M. D'Huyvetter, P. De Baetselier, G. Raes, T. Lahoutte and P. Matthys, SPECT Imaging of Joint Inflammation with Nanobodies Targeting the Macrophage Mannose Receptor in a Mouse Model for Rheumatoid Arthritis, *J. Nucl. Med. Off. Publ. Soc. Nucl. Med.*, 2013, 54(5), 807–814, DOI: 10.2967/jnumed.112.111781.
- 82 F. Zheng, S. Put, L. Bouwens, T. Lahoutte, P. Matthys, S. Muyltermans, P. De Baetselier, N. Devoogdt, G. Raes and S. Schoonooghe, Molecular Imaging with Macrophage CRIG-Targeting Nanobodies for Early and Preclinical Diagnosis in a Mouse Model of Rheumatoid Arthritis, *J. Nucl. Med. Off. Publ. Soc. Nucl. Med.*, 2014, 55(5), 824–829, DOI: 10.2967/jnumed.113.130617.
- 83 A. Verhelle, W. Van Overbeke, C. Peleman, R. De Smet, O. Zwaenepoel, T. Lahoutte, J. Van Dorpe, N. Devoogdt and J. Gettemans, Non-Invasive Imaging of Amyloid Deposits in a Mouse Model of AGel Using 99mTc-Modified Nanobodies and SPECT/CT, *Mol. Imaging Biol.*, 2016, 18(6), 887–897, DOI: 10.1007/s11307-016-0960-y.
- 84 K. De Groeve, N. Deschacht, C. De Koninck, V. Caveliers, T. Lahoutte, N. Devoogdt, S. Muyltermans, P. De Baetselier and G. Raes, Nanobodies as Tools for in Vivo Imaging of Specific Immune Cell Types, *J. Nucl. Med. Off. Publ. Soc. Nucl. Med.*, 2010, 51(5), 782–789, DOI: 10.2967/jnumed.109.070078.
- 85 K. Broos, M. Keyaerts, Q. Lecocq, D. Renmans, T. Nguyen, D. Escors, A. Liston, G. Raes, K. Breckpot and N. Devoogdt, Non-Invasive Assessment of Murine PD-L1 Levels in Syngeneic Tumor Models by Nuclear Imaging with Nanobody Tracers, *Oncotarget*, 2017, 8(26), 41932–41946, DOI: 10.18632/oncotarget.16708.
- 86 A. Broisat, S. Hernot, J. Toczec, J. De Vos, L. M. Riou, S. Martin, M. Ahmadi, N. Thielens, U. Wernery, V. Caveliers, S. Muyltermans, T. Lahoutte, D. Fagret, C. Ghezzi and N. Devoogdt, Nanobodies Targeting Mouse/Human VCAM1 for the Nuclear Imaging of Atherosclerotic Lesions, *Circ. Res.*, 2012, 110(7), 927–937, DOI: 10.1161/CIRCRESAHA.112.265140.
- 87 A. Broisat, J. Toczec, L. S. Dumas, M. Ahmadi, S. Bacot, P. Perret, L. Slimani, G. Barone-Rochette, A. Soubies, N. Devoogdt, T. Lahoutte, D. Fagret, L. M. Riou and C. Ghezzi, 99mTc-CaVCAM1-5 Imaging Is a Sensitive and Reproducible Tool for the Detection of Inflamed Atherosclerotic Lesions in Mice, *J. Nucl. Med. Off. Publ. Soc. Nucl. Med.*, 2014, 55(10), 1678–1684, DOI: 10.2967/jnumed.114.143792.
- 88 L. S. Dumas, F. Briand, R. Clerc, E. Brousseau, C. Montemagno, M. Ahmadi, S. Bacot, A. Soubies, P. Perret, L. M. Riou, N. Devoogdt, T. Lahoutte, G. Barone-Rochette, D. Fagret, C. Ghezzi, T. Sulpice and A. Broisat, Evaluation of Antiatherogenic Properties of Ezetimibe Using 3H-Labeled Low-Density-Lipoprotein Cholesterol and 99mTc-CaVCAM1-5 SPECT in ApoE<sup>-/-</sup> Mice Fed the Paigen Diet, *J. Nucl. Med. Off. Publ. Soc. Nucl. Med.*, 2017, 58(7), 1088–1093, DOI: 10.2967/jnumed.116.177279.
- 89 G. Bala, H. Baudhuin, I. Remory, K. Gillis, P. Debie, A. Krasniqi, T. Lahoutte, G. Raes, N. Devoogdt, B. Cosyns and S. Hernot, Evaluation of [99mTc]Radiolabeled Macrophage Mannose Receptor-Specific Nanobodies for Targeting of Atherosclerotic Lesions in Mice, *Mol. Imaging Biol.*, 2018, 20(2), 260–267, DOI: 10.1007/s11307-017-1117-3.
- 90 B. M. Zeglis and J. S. Lewis, A Practical Guide to the Construction of Radiometallated Bioconjugates for Positron Emission Tomography, *Dalton Trans. Camb. Engl.* 2003, 2011, 40(23), 6168–6195, DOI: 10.1039/c0dt01595d.
- 91 M. Kijanka, B. Dorresteijn, S. Oliveira and P. M. P. van Bergen en Henegouwen, Nanobody-Based Cancer Therapy of Solid Tumors, *Nanomed.*, 2015, 10(1), 161–174, DOI: 10.2217/nnm.14.178.
- 92 I. Jovčevska and S. Muyltermans, The Therapeutic Potential of Nanobodies, *BioDrugs Clin. Immunother. Biopharm. Gene Ther.*, 2020, 34(1), 11–26, DOI: 10.1007/s40259-019-00392-z.
- 93 C. Xavier, A. Blykers, I. Vaneycken, M. D'Huyvetter, J. Heemskerk, T. Lahoutte, N. Devoogdt and V. Caveliers, 18F-Nanobody for PET Imaging of HER2 Overexpressing Tumors, *Nucl. Med. Biol.*, 2016, 43(4), 247–252, DOI: 10.1016/j.nucmedbio.2016.01.002.
- 94 G. Vaidyanathan, D. McDougald, J. Choi, E. Koumariou, D. Weitzel, T. Osada, H. K. Lyrly and M. R. Zalutsky, Preclinical Evaluation of 18F-Labeled Anti-HER2 Nanobody Conjugates for Imaging HER2 Receptor Expression by Immuno-PET, *J. Nucl. Med. Off. Publ. Soc. Nucl. Med.*, 2016, 57(6), 967–973, DOI: 10.2967/jnumed.115.171306.
- 95 A. Krasniqi, M. D'Huyvetter, C. Xavier, K. Van der Jeught, S. Muyltermans, J. Van Der Heyden, T. Lahoutte, J. Tavernier and N. Devoogdt, Theranostic Radiolabeled Anti-CD20 SdAb for Targeted Radionuclide Therapy of Non-Hodgkin Lymphoma, *Mol. Cancer Ther.*, 2017, 16(12), 2828–2839, DOI: 10.1158/1535-7163.MCT-17-0554.
- 96 M. J. W. D. Vosjan, J. Vercammen, J. A. Kolkman, M. Stigter-van Walsum, H. Revets and G. A. M. S. van Dongen, Nanobodies Targeting the Hepatocyte Growth Factor: Potential New Drugs for Molecular Cancer Therapy,



- Mol. Cancer Ther.*, 2012, **11**(4), 1017–1025, DOI: 10.1158/1535-7163.MCT-11-0891.
- 97 M. Keyaerts, C. Xavier, J. Heemskerk, N. Devoogdt, H. Everaert, C. Ackaert, M. Vanhoeij, F. P. Duhoux, T. Gevaert, P. Simon, D. Schallier, C. Fontaine, I. Vaneycken, C. Vanhove, J. De Greve, J. Lamote, V. Caveliers and T. Lahoutte, Phase I Study of <sup>68</sup>Ga-HER2-Nanobody for PET/CT Assessment of HER2 Expression in Breast Carcinoma, *J. Nucl. Med. Off. Publ. Soc. Nucl. Med.*, 2016, **57**(1), 27–33, DOI: 10.2967/jnumed.115.162024.
- 98 C. Xavier, A. Blykers, D. Laoui, E. Bolli, I. Vaneyken, J. Bridoux, H. Baudhuin, G. Raes, H. Everaert, K. Movahedi, J. A. Van Ginderachter, N. Devoogdt, V. Caveliers, T. Lahoutte and M. Keyaerts, Clinical Translation of [<sup>68</sup>Ga]Ga-NOTA-Anti-MMR-SdAb for PET/CT Imaging of Protumorigenic Macrophages, *Mol. Imaging Biol.*, 2019, **21**(5), 898–906, DOI: 10.1007/s11307-018-01302-5.
- 99 A. Blykers, S. Schoonoghe, C. Xavier, K. D'hoë, D. Laoui, M. D'Huyvetter, I. Vaneycken, F. Cleeren, G. Bormans, J. Heemskerk, G. Raes, P. De Baetselier, T. Lahoutte, N. Devoogdt, J. A. Van Ginderachter and V. Caveliers, PET Imaging of Macrophage Mannose Receptor-Expressing Macrophages in Tumor Stroma Using <sup>18</sup>F-Radiolabeled Camelid Single-Domain Antibody Fragments, *J. Nucl. Med. Off. Publ. Soc. Nucl. Med.*, 2015, **56**(8), 1265–1271, DOI: 10.2967/jnumed.115.156828.
- 100 M. Rashidian, E. J. Keliher, A. M. Bilate, J. N. Duarte, G. R. Wojtkiewicz, J. T. Jacobsen, J. Cragolini, L. K. Swee, G. D. Vitoria, R. Weissleder and H. L. Ploegh, Noninvasive Imaging of Immune Responses, *Proc. Natl. Acad. Sci. U. S. A.*, 2015, **112**(19), 6146–6151, DOI: 10.1073/pnas.1502609112.
- 101 C. H. M. J. Van Elssen, M. Rashidian, V. Vrbanac, K. W. Wucherpennig, Z. E. Habre, J. Sticht, C. Freund, J. T. Jacobsen, J. Cragolini, J. Ingram, L. Plaisier, E. Spierings, A. M. Tager and H. L. Ploegh, Noninvasive Imaging of Human Immune Responses in a Human Xenograft Model of Graft-Versus-Host Disease, *J. Nucl. Med. Off. Publ. Soc. Nucl. Med.*, 2017, **58**(6), 1003–1008, DOI: 10.2967/jnumed.116.186007.
- 102 M. Rashidian, M. W. LaFleur, V. L. Verschoor, A. Dongre, Y. Zhang, T. H. Nguyen, S. Kolifraht, A. R. Aref, C. J. Lau, C. P. Paweletz, X. Bu, G. J. Freeman, M. I. Barrasa, R. A. Weinberg, A. H. Sharpe and H. L. Ploegh, Immuno-PET Identifies the Myeloid Compartment as a Key Contributor to the Outcome of the Antitumor Response under PD-1 Blockade, *Proc. Natl. Acad. Sci. U. S. A.*, 2019, **116**(34), 16971–16980, DOI: 10.1073/pnas.1905005116.
- 103 J. R. Ingram, M. Dougan, M. Rashidian, M. Knoll, E. J. Keliher, S. Garrett, S. Garforth, O. S. Blomberg, C. Espinosa, A. Bhan, S. C. Almo, R. Weissleder, H. Lodish, S. K. Dougan and H. L. Ploegh, PD-L1 Is an Activation-Independent Marker of Brown Adipocytes, *Nat. Commun.*, 2017, **8**(1), 647, DOI: 10.1038/s41467-017-00799-8.
- 104 J. R. Ingram, O. S. Blomberg, M. Rashidian, L. Ali, S. Garforth, E. Fedorov, A. A. Fedorov, J. B. Bonanno, C. Le Gall, S. Crowley, C. Espinosa, T. Biary, E. J. Keliher, R. Weissleder, S. C. Almo, S. K. Dougan, H. L. Ploegh and M. Dougan, Anti-CTLA-4 Therapy Requires an Fc Domain for Efficacy, *Proc. Natl. Acad. Sci. U. S. A.*, 2018, **115**(15), 3912–3917, DOI: 10.1073/pnas.1801524115.
- 105 N. Jalkhani, J. R. Ingram, M. Rashidian, S. Rickelt, C. Tian, H. Mak, Z. Jiang, H. L. Ploegh and R. O. Hynes, Noninvasive Imaging of Tumor Progression, Metastasis, and Fibrosis Using a Nanobody Targeting the Extracellular Matrix, *Proc. Natl. Acad. Sci. U. S. A.*, 2019, **116**(28), 14181–14190, DOI: 10.1073/pnas.1817442116.
- 106 R. van der Meel, W. M. Gallagher, S. Oliveira, A. E. O'Connor, R. M. Schiffelers and A. T. Byrne, Recent Advances in Molecular Imaging Biomarkers in Cancer: Application of Bench to Bedside Technologies, *Drug Discovery Today*, 2010, **15**(3–4), 102–114, DOI: 10.1016/j.drudis.2009.12.003.
- 107 M. L. James and S. S. Gambhir, A Molecular Imaging Primer: Modalities, Imaging Agents, and Applications, *Physiol. Rev.*, 2012, **92**(2), 897–965, DOI: 10.1152/physrev.00049.2010.
- 108 M. Silindir-Gunay, E. T. Sarcan and A. Y. Ozer, Near-Infrared Imaging of Diseases: A Nanocarrier Approach, *Drug Dev. Res.*, 2019, **80**(5), 521–534.
- 109 M. M. Kijanka, A. S. A. van Brussel, E. van der Wall, W. P. T. M. Mali, P. J. van Diest, P. M. P. van Bergen En Henegouwen and S. Oliveira, Optical Imaging of Pre-Invasive Breast Cancer with a Combination of VHHs Targeting CAIX and HER2 Increases Contrast and Facilitates Tumour Characterization, *EJNMMI Res*, 2016, **6**(1), 14, DOI: 10.1186/s13550-016-0166-y.
- 110 A. S. A. van Brussel, A. Adams, S. Oliveira, B. Dorresteijn, M. El Khattabi, J. F. Vermeulen, E. van der Wall, W. P. T. M. Mali, P. W. B. Derksen, P. J. van Diest and P. M. P. van Bergen En Henegouwen, Hypoxia-Targeting Fluorescent Nanobodies for Optical Molecular Imaging of Pre-Invasive Breast Cancer, *Mol. Imaging Biol.*, 2016, **18**(4), 535–544, DOI: 10.1007/s11307-015-0909-6.
- 111 C. Chi, Y. Du, J. Ye, D. Kou, J. Qiu, J. Wang, J. Tian and X. Chen, Intraoperative Imaging-Guided Cancer Surgery: From Current Fluorescence Molecular Imaging Methods to Future Multi-Modality Imaging Technology, *Theranostics*, 2014, **4**(11), 1072–1084, DOI: 10.7150/thno.9899.
- 112 P. Debie, M. Vanhoeij, N. Poortmans, J. Puttemans, K. Gillis, N. Devoogdt, T. Lahoutte and S. Hernot, Improved Debulking of Peritoneal Tumor Implants by Near-Infrared Fluorescent Nanobody Image Guidance in an Experimental Mouse Model, *Mol. Imaging Biol.*, 2018, **20**(3), 361–367, DOI: 10.1007/s11307-017-1134-2.
- 113 G. D. Luker and K. E. Luker, Optical Imaging: Current Applications and Future Directions, *J. Nucl. Med. Off. Publ. Soc. Nucl. Med.*, 2008, **49**(1), 1–4, DOI: 10.2967/jnumed.107.045799.
- 114 A. Hellebust and R. Richards-Kortum, Advances in Molecular Imaging: Targeted Optical Contrast Agents for Cancer Diagnostics, *Nanomed.*, 2012, **7**(3), 429–445, DOI: 10.2217/nnm.12.12.



- 115 M. J. O'Connell, S. M. Bachilo, C. B. Huffman, V. C. Moore, M. S. Strano, E. H. Haroz, K. L. Rialon, P. J. Boul, W. H. Noon, C. Kittrell, J. Ma, R. H. Hauge, R. B. Weisman and R. E. Smalley, Band Gap Fluorescence from Individual Single-Walled Carbon Nanotubes, *Science*, 2002, **297**(5581), 593–596, DOI: 10.1126/science.1072631.
- 116 F. A. Mann, Z. Lv, J. Großhans, F. Opazo and S. Kruss, Nanobody-Conjugated Nanotubes for Targeted Near-Infrared *In Vivo* Imaging and Sensing, *Angew. Chem., Int. Ed.*, 2019, **58**(33), 11469–11473, DOI: 10.1002/anie.201904167.
- 117 N. K. Tafreshi, M. C. Lloyd, M. M. Bui, R. J. Gillies and D. L. Morse, Carbonic Anhydrase IX as an Imaging and Therapeutic Target for Tumors and Metastases, *Subcell. Biochem.*, 2014, **75**, 221–254, DOI: 10.1007/978-94-007-7359-2\_12.
- 118 J. Li, G. Zhang, X. Wang and X.-F. Li, Is Carbonic Anhydrase IX a Validated Target for Molecular Imaging of Cancer and Hypoxia?, *Future Oncol. Lond. Engl.*, 2015, **11**(10), 1531–1541, DOI: 10.2217/fon.15.11.
- 119 S. Massa, N. Vikani, C. Betti, S. Ballet, S. Vanderhaegen, J. Steyaert, B. Descamps, C. Vanhove, A. Bunschoten, F. W. B. van Leeuwen, S. Hernot, V. Cavelliers, T. Lahoutte, S. Muyltermans, C. Xavier and N. Devoogdt, Sortase A-Mediated Site-Specific Labeling of Camelid Single-Domain Antibody-Fragments: A Versatile Strategy for Multiple Molecular Imaging Modalities, *Contrast Media Mol. Imaging*, 2016, **11**(5), 328–339, DOI: 10.1002/cmml.1696.
- 120 T. M. Lwin, S. Hernot, H. Hollandsworth, S. Amirfakhri, F. Filemoni, P. Debie, R. M. Hoffman and M. Bouvet, Tumor-Specific near-Infrared Nanobody Probe Rapidly Labels Tumors in an Orthotopic Mouse Model of Pancreatic Cancer, *Surgery*, 2020, **168**(1), 85–91, DOI: 10.1016/j.surg.2020.02.020.
- 121 X. Fan, L. Wang, Y. Guo, Z. Tu, L. Li, H. Tong, Y. Xu, R. Li and K. Fang, Ultrasonic Nanobubbles Carrying Anti-PSMA Nanobody: Construction and Application in Prostate Cancer-Targeted Imaging, *PloS One*, 2015, **10**(6), e0127419, DOI: 10.1371/journal.pone.0127419.
- 122 Z. Yu, M. Hu, Z. Li, N. Dan Xu, L. Zhu, Y. Guo, Q. Liu, W. Lan, J. Jiang and L. Wang, Anti-G250 Nanobody-Functionalized Nanobubbles Targeting Renal Cell Carcinoma Cells for Ultrasound Molecular Imaging, *Nanotechnology*, 2020, **31**(20), 205101, DOI: 10.1088/1361-6528/ab7040.
- 123 M. Punjabi, L. Xu, A. Ochoa-Espinosa, A. Kosareva, T. Wolff, A. Murtaja, A. Broisat, N. Devoogdt and B. A. Kaufmann, Ultrasound Molecular Imaging of Atherosclerosis With Nanobodies: Translatable Microbubble Targeting Murine and Human VCAM (Vascular Cell Adhesion Molecule) 1, *Arterioscler., Thromb., Vasc. Biol.*, 2019, **39**(12), 2520–2530, DOI: 10.1161/ATVBAHA.119.313088.
- 124 A. D'Hollander, H. Jans, G. V. Velde, C. Verstraete, S. Massa, N. Devoogdt, T. Stakenborg, S. Muyltermans, L. Lagae and U. Himmelreich, Limiting the Protein Corona: A Successful Strategy for *In Vivo* Active Targeting of Anti-HER2 Nanobody-Functionalized Nanostars, *Biomaterials*, 2017, **123**, 15–23, DOI: 10.1016/j.biomaterials.2017.01.007.
- 125 T. W. M. De Groof, V. Bobkov, R. Heukers and M. J. Smit, Nanobodies: New Avenues for Imaging, Stabilizing and Modulating GPCRs, *Mol. Cell. Endocrinol.*, 2019, **484**, 15–24, DOI: 10.1016/j.mce.2019.01.021.
- 126 S. Khaleghi, F. Rahbarizadeh, D. Ahmadvand and H. R. M. Hosseini, Anti-HER2 VHH Targeted Magnetoliposome for Intelligent Magnetic Resonance Imaging of Breast Cancer Cells, *Cell. Mol. Bioeng.*, 2017, **10**(3), 263–272, DOI: 10.1007/s12195-017-0481-z.
- 127 A. M. Prantner, C. Yin, K. Kamat, K. Sharma, A. C. Lowenthal, P. B. Madrid and N. Scholler, Molecular Imaging of Mesothelin-Expressing Ovarian Cancer with a Human and Mouse Cross-Reactive Nanobody, *Mol. Pharm.*, 2018, **15**(4), 1403–1411, DOI: 10.1021/acs.molpharmaceut.7b00789.
- 128 D. Shahbazi-Gahrouei and M. Abdolahi, Detection of MUC1-Expressing Ovarian Cancer by C595 Monoclonal Antibody-Conjugated SPIONs Using MR Imaging, *Scientific WorldJournal*, 2013, **2013**, 609151, DOI: 10.1155/2013/609151.

